Global and Planetary Change
June 2023, Volume 225, Pages 104118 (21p.)
https://doi.org/10.1016/j.gloplacha.2023.104118
https://archimer.ifremer.fr/doc/00833/94508/

Contourite depositional systems offshore Madeira Island: Decoding the deepwater circulation since the late cretaceous to the Quaternary in the NE-Central Atlantic

Roque C. [1, 2, *], Hernández-Molina J. [3], Brito P. [4], Madureira P. [1, 5], Quartau R. [2, 6], Magalhães V. [2, 4], Carrara G. [7]

[1] EMEPC - Estrutura de Missão para a Extensão da Plataforma Continental, Paço de Arcos 2770-047, Portugal
[2] Instituto Dom Luiz, University of Lisbon, Campo Grande, Lisbon 1749-016, Portugal
[3] Department Earth Sciences, Royal Holloway University London, Egham, Surrey TW20 0EX, United Kingdom
[4] Instituto Português do Mar e da Atmosfera, Divisão de Geologia Marinha e Georecursos, Lisbon, Portugal
[5] Department of Geosciences and Institute of Earth Sciences, University of Évora, Évora 7000, Portugal
[6] Instituto Hidrográfico, Divisão de Geologia Marinha, Lisbon, Portugal
[7] National Research Council, CNR Institute for Microelectronic and Microsystems, Bologna, Italy

* Corresponding author : C. Roque, email address : croque@emepc-portugal.org

Abstract :

There is still a great unawareness about the deep-water circulation in the NE-Central Atlantic since the Late Cretaceous. The morphology, sedimentary stacking pattern and distribution of contourite depositional systems have been widely used as paleoceanographic indicators, given clues about the relative velocity and pathways of bottom currents past-circulation. We present here evidence of a newcontourite features developed in the NE-Central Atlantic offshore Madeira Island between ~3000 m and ~ 4950 m water depth. These features allowed us to define two Contourite Depositional Systems (CDSs). The dataset used in our work iscomposed of multichannel reflection seismic profiles and DSDP and ODP sites for the chronostratigraphic framework. The seismic stratigraphy analysis allowed the identification ofsix seismic units (U1–U6) and a sub-unit (U6a) separated by erosional discontinuities (D1–D6). The acoustic basement corresponds to oceanic crust located in the Cretaceous Magnetic Quite Zone (~120 Ma to 84 Ma), but basalts drilled at DSDP Site 136 near Madeira Island indicate an age of about 106 Ma. Sedimentary deposits from seismic units are interpreted as pelagic (unit U1; Early Cretaceous); contourite (U2 to U6; Late Cretaceous to Quaternary); and mass transport deposits (U6a; Quaternary). These seismic units characterize the CDSs from Late Cretaceous (Campanian?), resting unconformably on pelagic sediments of probable Aptian to Santonian age. The CDS-1 (U2 to U4) was formed from Late Cretaceous (Campanian?) to Middle Miocene and the CDS-2 (U5 and U6) was deposited from Middle Miocene to Quaternary. They are bounded by major erosional surfaces and characterized by giant elongated mounded contourite drifts (Drift 1 and Drift 2, respectively). Presently, CDS-1 is inactive and buried by pelagic sediments. Conversely, CDS-2 outcrops between~3000 and 4800 m waterdepth on the lower slope of Madeira plateau. These results reveal that this region of the NE-Central Atlantic has been

swept by long-term northward bottom currents. We propose that the most plausible water masses responsible for these bottom-currents and drifts generation have been the Southern Component Water (SCW) and more recently the Antarctic Bottom Water (AABW). Consequently, the onset of the first incursion of the SCW was near the end of Late Cretaceous, probably in the Campanian. Since the late Eocene the AABW would have a dominant role in this region of the NE-Central Atlantic. Assuming that during cool periods, the AABW had a greater volume and circulated shallower than 4000 m, we hypothesized that CDS-2 has been mainly active during these periods. On the contrary, during warmer periods, the AABW circulates deeper (>4000 m) and thus contourite deposition associated with the AABW shifted to deeper water depths. Presently the CDS-2 can be considered as a relict feature. Therefore, the Madeira CDCs represents a unique and very promising sedimentary archive for reconstructing deep-water masses circulation and their variability in the NE-Central Atlantic since the end of Cretaceous through the Quaternary, where the oceanic seafloor irregularities have been key in controlling the water masses and bottom currents behavior.

Highlights

► Discovery of two contourite drift systems (CDS-1, CDS-2) in the Central NE-Atlantic. ► The CDS-1 recorded the circulation of SCW from Late Cretaceous to Miocene. ► The CDS-2 was formed by circulation of the AABW since the Miocene.

Keywords : oceanic island, contourite features, drift, Southern Component Water, Antarctic Bottom Water, Late Cretaceous, Quaternary

1. Introduction

The paleoceanography of the Central Atlantic since the end of Cretaceous remains poorly known (e.g., Hay, 2008; Murphy and Thomas, 2013; Donnadieu et al., 2016). Main uncertainties still persist regarding the timing of the onset, evolution, intensity, regional distribution, sources and pathways of deepwater masses. It is widely accepted that the full opening of the Equatorial Atlantic Gateway (EAG) in the Campanian (84-72 Ma) had a profound consequence in the reorganization of Atlantic deepwater circulation, allowing the connection between South and North Atlantic (Granot and Dyment, 2015; Poulsen et al., 2001; Martin et al., 2012; Robinson and Vance et al., 2012; Murphy and Thomas, 2013; Voigt et al., 2013; Donnadieu et al., 2016; Pérez-Díaz and Eagles, 2017). Kinematic reconstructions and numerical modeling of deepwater masses circulation indicate that by the Late Campanian-Maastrichtian deepwater exchange between the two basins was already established (e.g., Pérez-Díaz and Eagles, 2017). The present knowledge of these earlier deepwater masses characteristics and sources was derived mostly from neodymium isotopes signatures measured in fish teeth (e.g., Robinson and Vance, 2012; Thomas et al., 2013). These studies draw a complex scenario for the Late Cretaceous circulation, involving multiple sources of deep-water masses with variable influence and distribution (e.g., Martin et al., 2012; Robinson and Vance, 2012; Moiroud et al., 2016; Donnadieu et al., 2016). Since the end of Cretaceous throughout the Paleogene, the deep-water circulation in the Atlantic was dominated by a northward flowing water mass sourced in the Southern Ocean, the Southern Component Water (SCW), considered as an analogue to the modern-day Antarctic Bottom Water (AABW) (e.g, Hay, 2008; Sher and Martin, 2008). Other reliable and extensively used proxy to unravel deepwater circulation and bottom-current activity is the presence of contourite features in the geological record (e.g., Rebesco et al., 2014). Contourites are sediments deposited or substantially reworked by the persistent action of alongslope bottom currents (e.g., Stow et al., 2002; Rebesco et al., 2014). The continued circulation of these currents though time led to the accumulation of extensive (hundreds of kms) and thick sedimentary bodies (thousands of meters) called contourite drifts (Heezen and

Hollister, 1964; Hollister and Heezen 1972). Due to their high sedimentation rates (3-30 cm ka^{-1}) these contouritedeposits are considered a valuable high-resolution sedimentological archive and have been successfully used in paleoclimatic and paleoceanographic studies (e.g., Knutz, 2008; Rebesco and Camerlenghi, 2008, Rebesco et al., 2014). The major erosional surfaces and hiatuses found within its sedimentary record document major paleoceanographic and/or tectonic changes linked to the onset, evolution and eventually burial of drifts because of water masses circulation initiation, enhance and inactivation or displacement (Hernández-Molina et al., 2022). Moreover, changes on contourite drifts' sedimentary stacking pattern, acoustic facies, configuration, morphology and location can give valuable insights about bottom currents pathways, variability and intensity (e.g., Rebesco and Camerlenghi, 2008; Rebesco et al., 2014; Martorelli et al., 2021). Global contourite drifts distribution show that they concentrate mainly along continental margins and neighborhood areas, being less represented in deep oceanic basins (Rebesco et al., 2014; Thran et al., 2018). Actually, the majority of modern and fossil contourite drifts have been found along the Eastern and Western Atlantic continental margins, testifying major changes in paleoceanographic circulation (Thran et al., 2018). Among them, the oldest contourite drifts (Albian-Cenomanian) occur along the NE-African (Mourlot et al., 2018) and West Iberia (Soares et al., 2014) continental margins but probably were deposited from different water masses. In the Western Atlantic, the accumulation of contourite drifts seems to have started by the end of Cretaceous, although incipiently and locally (Mountain and Miller, 1992; Campbell and Mosher, 2016; Boyle et al., 2017; Rodrigues et al., 2022). The contourite drifts accumulation increased in both Atlantic basins since the Eocene (Campbell and Mosher, 2016; Boyle et al., 2017) and several continued to develop until the Quaternary. Comparatively, the occurrence of contourite drifts along the slope of oceanic islands is poorly documented and studied.

The Madeira Island located in the NE-Central Atlantic is a good target to study these depositional processes. It is at about 700 km NW from the African continental margin (Fig. 1), and the earliest reference to bottom-currents sweeping its western lower slope was presented by Heezen et al. (1959). Almost two decades later, Embley et al. (1978) studied this area with more

detail, identifying a wide feature reworked by bottom currents (Fig. 2). In the following decades, research has been focused mostly on the study of the turbidite systems developed southward of Madeira Island (e.g., Wynn et al., 2000; Talling et al., 2007; Hunt et al., 2013; Steverson et al., 2013). An exception was the study by Hernández-Molina et al. (2011) that predicted the presence of contourite drifts westward of Madeira Island based on numerical modeling of water masses circulation. This prediction was confirmed with the identification of a large contourite drift called Madeira Drift (~385 km long; ~175 km wide), between approximately 3000 m and 4800 m water depth (Roque et al., 2015, 2022). The westernmost part of Madeira Drift coincides with the area surveyed by Embley et al. (1978). In its vicinity and below 4800 m water depth, a large field of small patch drifts developed due to the interaction of the AABW with seafloor highs has been recently discovered (Roque et al., 2022).

The western slope of Madeira Island represents an unique and promising site to investigate the evolution of deep-water circulation and related deposits in this region of the NE-Central Atlantic because is: 1) an almost unexplored area regarding bottom currents activity, 2) located in an open ocean setting far away from continental margins influence, and 3) in the pathway of the two global deep-water masses, i.e. the North Eastern Atlantic Deep Water (NEADW) and AABW (Fig. 1a). The aims of this work are i) determine a seismic stratigraphic model for the contourite drift succession offshore Madeira Island based on multichannel seismic reflection data, ii) propose a sedimentary model since the Late Cretaceous to the Quaternary; and iii) decode the key evolutionary and paleoceanographic stages and evaluate their implications for the NE-Central Atlantic.

2. Geological and oceanographic settings

The Madeira Island is the largest one from the Madeira archipelago located in the Northeast Central Atlantic (Fig. 1). This island and its submarine edifice (hereafter called Madeira plateau) were generated on the African plate by alkaline intraplate volcanism related to the mantle plume upwelling activity (Geldmacher and Hoernle, 2000; Geldmacher et al., 2001; 2005; Schwarz et al., 2005), which produced a thermal regional swell (Sleep, 1990). This volcanic edifice was emplaced

on the early Cretaceous oceanic crust (e.g., Bird et al., 2007; Müller et al., 2008), and consists of basaltic tholeiitic diabase rocks moderately serpentinized and typical of oceanic basement (layer 2) (Hayes et al., 1972). The seamount stage of Madeira Island may have begun later, near the Paleocene-Eocene boundary (Schmincke, 1982; Hoernle et al., 1995), although the precise age is still undetermined. The Madeira Island reached the shield stage with subaerial volcanic activity in the Late Miocene around 7.0-5.6 Ma, after several uplift episodes (Ramalho et al., 2015). The main phase of this volcanic activity started at 5.6 and ended at 3.0 Myr ago (Mata et al., 2013; Matos et al., 2015), but periods of minor activity occurred at 740 ka, 620 ka, 550 ka and 6.5 ka (Ribeiro and Ramalho, 2007).

The oldest marine sediments recovered nearby the Madeira Island consists of calcareous (nannofossil) oozes (chalk) of Aptian age, covered by Late Aptian to Early Cenomanian clays and red clays interbedded with layers of volcanic ash of Cenonian-Albian age (Hayes et al., 1972) (Fig. 3). The Cretaceous sedimentary succession is separated by a 60 Myr hiatus from Early Miocene silty clay. The overlying Early Miocene to Early Pliocene corresponds to nannofossil oozes and calcareous mud, The Late Quaternary sedimentation consisted entirely of calcareous mud and calcareous ooze with low deposition rates (1.5 cm ka^{-1}) (Embley et al., 1978). The occurrence of interbedded volcanogenic sand layers is restricted to the southeastern area surrounding the Madeira plateau (Embley et al. 1978) and is linked to the Madeira Turbidite System (Stevenson et al., 2013) (Fig. 1b).

The oceanographic framework around Madeira Island is still poorly known and thus only a regional picture can be given (e.g., Pinet, 2011) (Fig. 1a). Near-surface circulation is governed by currents associated with the eastern part of the anticyclonic North Atlantic subtropical gyre, which northern boundary is the Azores Current (AC) with temperature and salinity, respectively, of 15º and 36.4‰. (Stramma, 2001; Comas-Rodríguez et al., 2011). The eastward-flowing ACseparates into three branches near 33º N. Two branches diverge west of Madeira and flow into the Gulf of Cadiz (e.g., Vargas et al., 2003) and along the western Iberian margin as the Iberian Poleward Current (Peliz et al., 2005). The third branch recirculate southwardand feed the Canary Current

(Barton, 2001; Stramma, 2001). The intermediate circulation is represented by the Eastern North Atlantic Central Water (ENACW) and the Antarctic Intermediate Water (AAIW). The core of the ENACW circulates above 500 m depth, i.e. within the ACregion (e.g., Fründt and Waniek, 2012). The ENACW has a temperature and salinity, respectively, of 8.0º-18ºC and 35.2-36.7‰. The AAIW spreads from 500-700 m until 1500 m depth and reaches latitudes up to 36ºN (Roemmich and Wunsch, 1985; Steele et al., 2009; Louarn and Morin, 2011; Roque et al 2019). This water mass has its origin in the Antarctic Polar Frontal Zone (Steele et al., 2009) and is characterized by low temperatures (2.5º-5ºC), low salinity (33.8-34.6‰), very high nutrient and low oxygen concentrations (Tsuchiya et al., 1992; Arhan et al., 1994; Roque et al 2019). The deep-water circulation involves the Northeast Atlantic Deep Water (NEADW) and the Antarctic Bottom Water (AABW). The NEADW is a moderately cold (3º-4ºC) and salty (~34.9-35.0‰) deep-water mass that extends down to ~4000 m depth and moves toward south, although makes a gyre in Madeira Island and moves into the Gulf of Cadiz (Hernández-Molina et al., 2011). It is a mixture of water masses originated in the Nordic Seas, the Iceland Scotland Overflow Water (ISOW), the Labrador Sea Water (LSW), and minor traces of Mediterranean Outflow Water (MOW) and Lower Deep Water of Antarctic origin (van Aken, 1999; Glazkova et al., 2022). The eastern branch of NEADW passes the Charlie-Gibbs Fracture Zone and spreads southward into the Eastern Atlantic (Fleischmann et al., 2001; Smethie et al., 2000). The AABW originates in the Weddell and Ross Seas and dominates the water column below ~4000 m depth as it moves toward north. This water mass enters the equatorial eastern Atlantic through the Romanche and Vema fracture zones and circulates northwards along the African margin until it reaches the North Atlantic (Glazkova et al., 2022). A branch of AABW flows in this direction bathing the deeper part of the western Madeira Plateau and the western flank of the Madeira-Tore Rise. The AABW is characterized by very low temperature (-0.4º-1.7ºC) and salinity (34.6-34.7‰) and high carbonate corrosion (Glazkova et al., 2022).

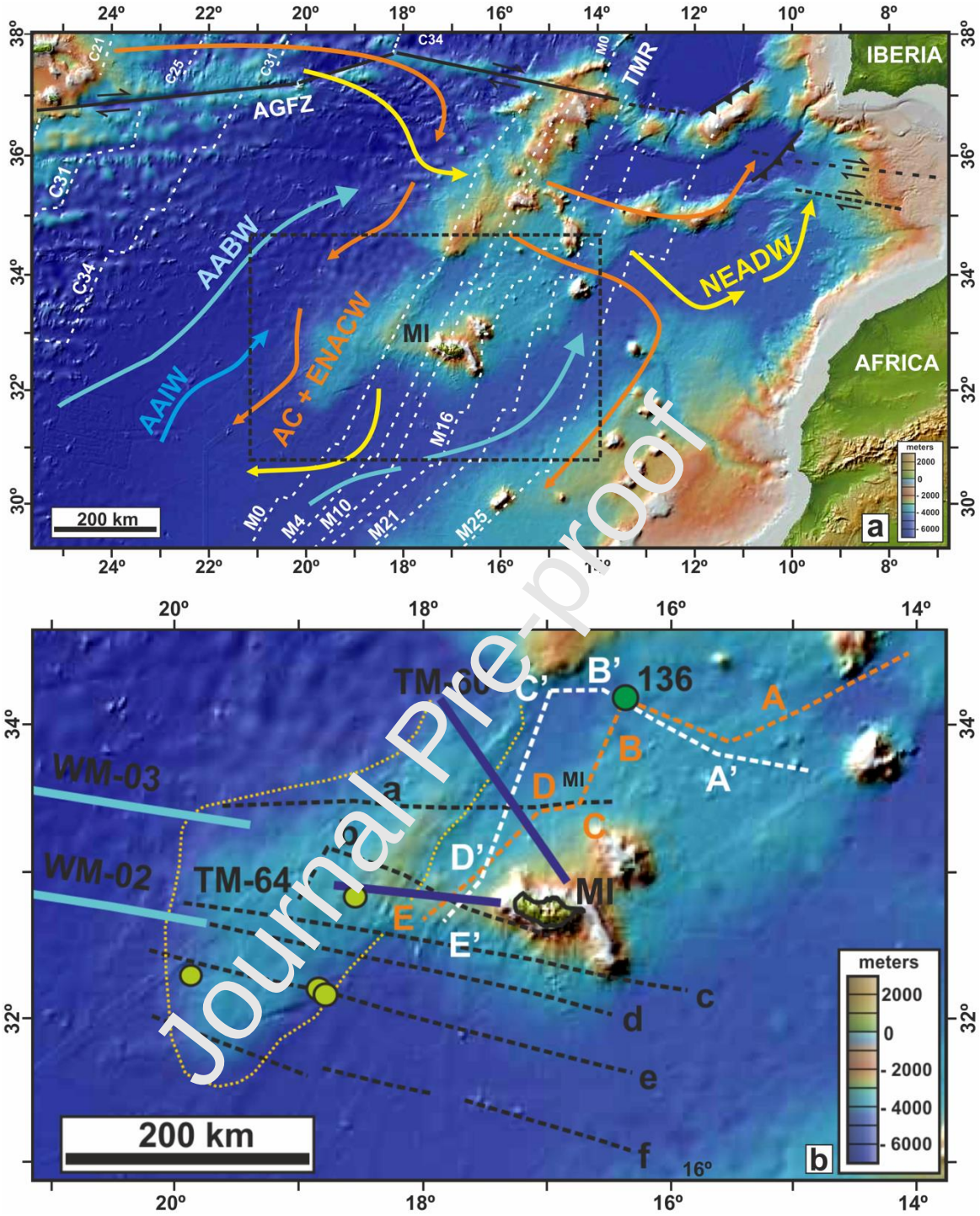

Figure 1 – a) Location of the Madeira Island (MI) in the context of the NE-Central Atlantic and main paths of water masses. AC= Azores Current; ENACW= Eastern North Atlantic Central Water; AAIW= Antarctica Intermediate Water; NEADW= Northeast Atlantic Deep Water; AABW= Antarctica Bottom Water. AGFZ= Azores Gibraltar Fracture Zone; TMR= Tore-Madeira Rise. The dashed white lines represent isochrons from M25 to C21. b) Dataset used in this study composed of multichannel seismic profiles WM (light blue) and TM (dark blue) and DSPS Site 136 (dark green circle). Location of published vintage seismic lines used to complement our data: seismic profiles from Embley et al. (1978) (dashed black lines) and from Hayes et al. (1972) (dashed orange and white lines). Olive green circles indicate the location of piston cores from Embley et al. (1978). Bathymetry from GeoMapApp (http://www.geomapapp.org).

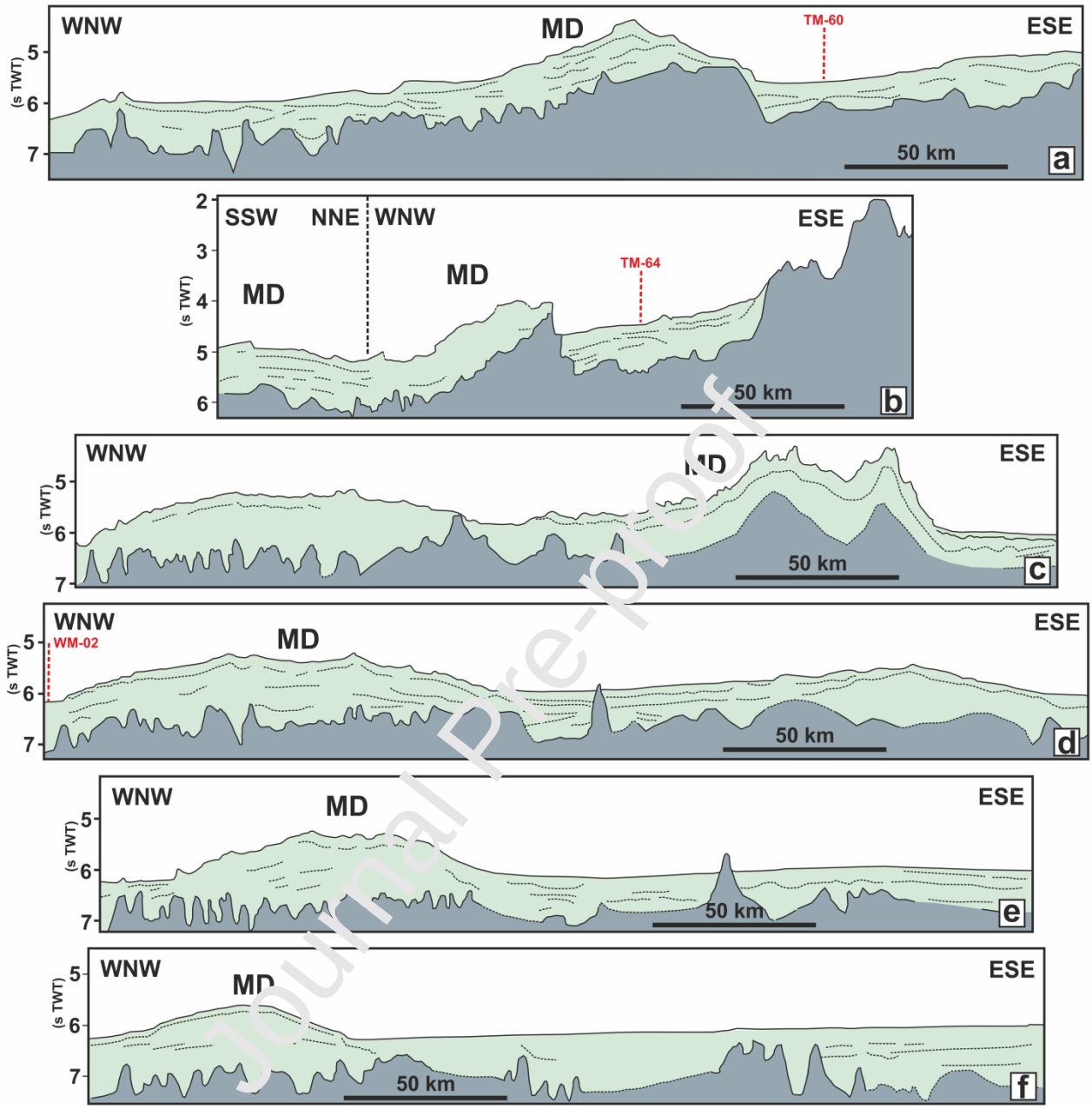

Figure 2 – Line drawing of seismic profiles (a to f) presented by Embley et al. (1978). The acoustic basement is shown in gray and the sedimentary cover in light green. The thick mounded body seen in the WNW part of these profiles corresponds to the Madeira Drift (MD), a giant contourite drift recognized offshore west Madeira Island first by Heezen et al. (1959) and later surveyed by Embley et al. (1978). The crossing with WM-02 and TM profiles is shown. (Seismic lines position in Fig. 1b).

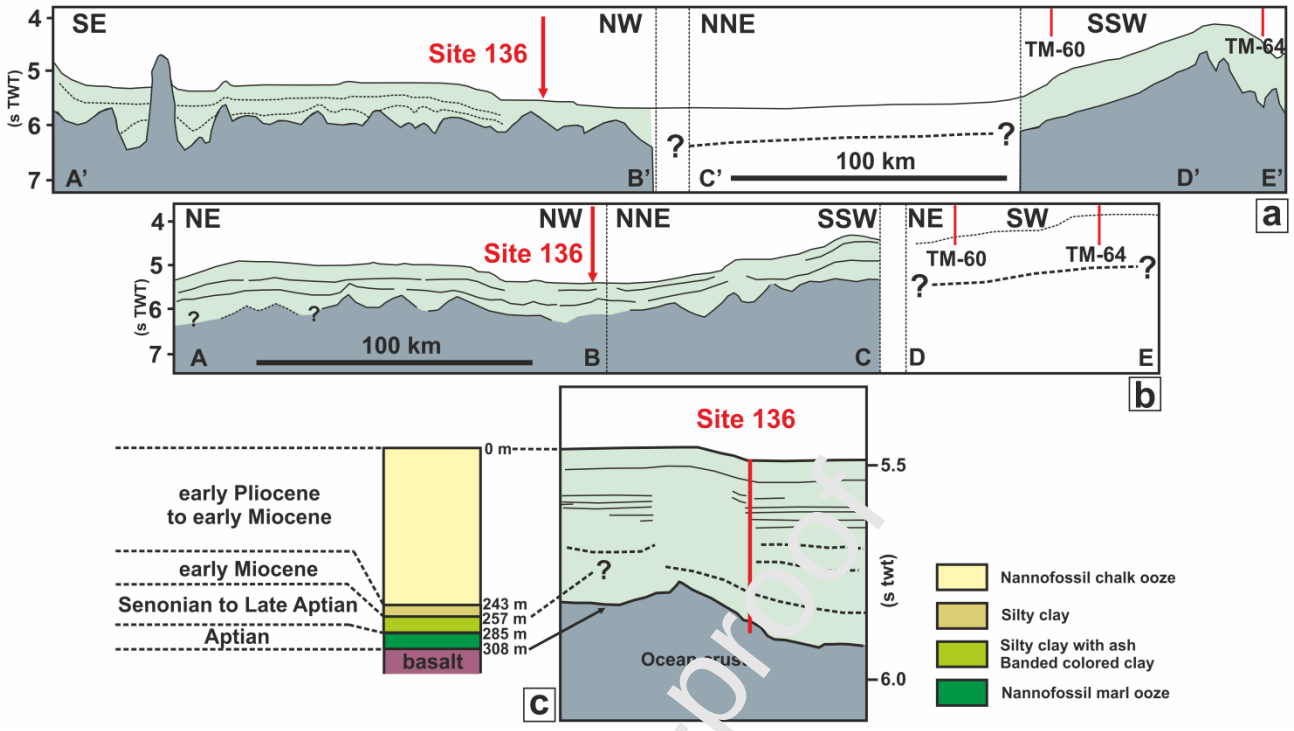

Figure 3 - a) and b) Line drawing of seismic profiles used for DSDP Site 136 drilling. Ocean crust is in dark gray and the sedimentary cover in light green (see Figure 1b for location). Crossing position with TM-60 and TM-64 profiles is shown. White areas in the profiles represent parts of very low-quality seismic record without clearly reflections. The inferred position of the interface basement-sedimentary cover is represented by the dashed black line with question marks. c) Lithostratigraphic column of Site 136 and correlation with seismic profile A'-B' (see Figure 1b for location). Note the existence of a hiatus between the Cretaceous and Miocene.

3. Paleoceanographic framework

The understanding of Cretaceous oceanic circulation remains limited and controversial, but is widely accepted that it was very distinct from the modern one (e.g., Otto-Bliesner et al., 2002; Friedrich et al., 2008; Hay, 2009; Robinson et al., 2010; MacLeod et al., 2011; Martin et al., 2012; Murphy and Thomas, 2013; Donnadieu et al., 2016). The Early Cretaceous was dominated by sluggish ocean circulation with little renewal of deepwater (Hay, 2009). This situation promoted anoxic and stagnant conditions around the continental margins with the widespread deposition of black shales (Föllmi, 2012; Jones et al., 2017). This happened mainly because the passages for deep-water in the North Atlantic were restricted to the Caribbean and Tethyan gateways (Voigt et al., 2013). This scenario changed in the Late Cretaceous driven by the opening of the Equatorial

Atlantic Gateway and subsidence of Walvis Ridge-Rio Grande Rise system (~100-83 Ma) (Föllmi, 2012; Robinson and Vance, 2012; Thibault et al., 2016; Huber et al., 2018). These events gave rise to a time marked by the termination of anoxia events, long-term climatic cooling, changes in deep-water circulation style promoted by the connection and deep-water exchange between South and North Atlantic basins (e.g., MacLeod et al., 2011; Friedrich et al., 2012; Martin et al., 2012; Granot and Dyment, 2015; Robinson and Vance, 2012; Murphy and Thomas, 2013; Voigt et al., 2013; Donnadieu et al., 2016; Mioroud et al., 2016; Pérez-Díaz and Eagles, 2017; Ladant et al., 2020). In the Campanian (84-72 Ma), the Equatorial Atlantic Gateway was fully opened favoring the progressive and better ventilated circulation between these two basins (Poulsen et al., 2001; Martin et al., 2012; Robinson and Vance et al., 2012; Murphy and Thomas, 2013; Voigt et al., 2013; Granot and Dyment, 2015; Donnadieu et al., 2016; Pérez-Díaz and Eagles, 2017). Therefore, since the Late Campanian-Maastrichtian the ocean circulation involved a more oxygenated deep-water mass sourced in the south ocean, the SCW (MacLeod et al., 2011; Friedrich et al., 2012; Murphy and Thomas, 2013; Sabatino et al., 2018; Ladant et al., 2020; Palcu et al., 2020). This water mass crossed the Equatorial Atlantic Gateway and spread northward bathing the entire Atlantic basin at depths greater than 3000 m (Robinson and Vance, 2012; Donnadieu et al., 2016; Pérez-Díaz and Eagles, 2017; Ladant et al., 2020).

The Cenozoic has been a period punctuated by major plate reorganization with the opening and deepening gateways as the Tasmanian Gateway and the Drake Passage and consequent changes in oceanic basins connectivity (e.g., Wright and Miller, 1993; Sher and Martin, 2006; Potter and Szatmari, 2009; Sher et al., 2015). These events led to the establishment of a new oceanic circulation patterns and have been pointed out as the main responsible for driving the profound climate changes that marked the Cenozoic (e.g., Lawver and Gahagan, 2003; Huber et al., 2004; Huber and Nof, 2006; Bahr et al., 2022). During the Paleocene, the SCW remained as the single deep-water mass flowing in the Atlantic basin (e.g., Sykes et al., 1998; Thomas et al., 2003). Widespread seafloor erosion during the Late Paleocene testifies a vigorous SCW flowing in the Atlantic (Mountain and Miller, 1992). The enhancement of the SCW occurred after the development

of the deep Antarctic water mass due to the deep opening of the Tasmanian Gateway around 47 Ma (Bahr et al., 2022) later enhanced because of the opening and of the Drake Passage in the late Eocene (Lawver and Gahagan, 2003; Sher and Martin, 2006; Livermore et al., 2007; Lagabrielle et al., 2009; Straume et al., 2020; Toumoulin et al., 2020; Bahr et al., 2022). The production and strengthening of this water mass was coeval with the initiation of the emplacement and expansion of the East Antarctica ice sheet in the earliest Oligocene (Zachos et al., 2001; Lower and Gahagan, 2003; Diekmann et al., 2004; Miller et al., 2005; Huber and Nof, 2006; Miller et al., 2009; Borrelli et al., 2014; Moebius et al., 2014; Hutchinson et al., 2020; Zhang et al., 2021). Both passages deepened throughout the Oligocene allowing a better connection and deep-water exchange between basins. Several hiatuses found in the Southern Ocean testify intervals of enhanced SCW in the Late Eocene (~40 Ma), earliest Oligocene (~36 Ma) middle Oligocene (~30 Ma) and latest Oligocene (~24 Ma) (Wright and Miller, 1993).

The middle to late Miocene was marked by a global cooling as consequence of substantial expansion of East and West Antarctic ice sheets (e.g., Zachos et al., 2001; Billups 2002; Miller et al., 2005; Potter and Szatmari, 2009). These conditions promoted the enhancement of the AABW (Hall et al., 2003) that started after the opening of the Drake Passage (Bahr et al., 2022). It remained as the dominant deep-water mass during the middle Miocene and the densest one since then (Huang et al., 2017). After the uplift and closure of the Isthmus of Panama at 2.5-3.0 Ma, a circulation pattern similar to the modern one was established with the strengthening of the NADW in the Late Miocene (e.g., Wright et al., 1991; Haug and Tiedemann, 1998; Nisancioglu et al., 2003). The AABW circulation slowed down since this time (Hassold et al., 2009) but had periods of intensification during the Quaternary (Sykes et al., 1998).

The Quaternary was dominated by alternating glacial and interglacial cycles that imposed severe changes in the deep-water circulation (e.g., Bell et al., 2015). Several studies indicate reduction, or even suppression, of NADW formation during glacial periods (e.g., Emery and Uchupi, 1984; Raymo et al., 1996; Ravelo and Andreasen, 2000; Luo et al., 2018). Thus, stronger exportof NADW occurred during interglacial conditions, with a major peak recognized at ~2.0-1.5 Ma (Bell et al.,

2015). In opposition, glacial periods were marked by production and spreading of invigorated, faster, saltier and voluminous AABW (Boyle and Keigwin, 1987; Duplessy et al., 1988; Lund et al., 2011). Moreover, several authors proposed that the AABW-NADW boundary, presently at ~4000 m depth, was located at around 2000 m depth during the Last Glacial Maximum (LGM) (Lund et al., 2011; Adkins, 2013; Böhm et al., 2015; Matsumoto, 2017).

4. Material and methods

The dataset used in this work is composed of multichannel seismic reflection profiles (Fig. 1b). Seismic reflection profiles TM60 and TM64 were acquired by IFREMER in 2001 during the Tore-Madère scientific survey (Cornen et al., 2003) and available at https://campagnes.flotteocenographic.fr. In this cruise, a SISRAP system (by Genavir) composed of a 6-channel seismic streamer, 590 m long was used. Two GI-GUN in harmonic mode (300 in^3) was used as seismic source. The near offset was 213 m and the shot interval 50 m. Seismic record was 10 s TWT with a 4 ms sample rate. SISRAP system is commonly used to acquire single channel profiles at high cruise speed (8-10 knots). Seismic reflection profiles WM-02 and WM-03 (Fig. 1b) were acquired in 2006 onboard the *R/V Akademik Shatskiy* using a 5720 in^3 bolt gun array, a streamer of 7950 m length, deployed at 9 m depth, with a group interval of 12.50 m, 636 channels and a shooting distance of 50 m. The recording parameters used a high cut filter of 200 Hz 370 dB/Oct; a sample interval of 2 ms; and a record length of 18128 ms. The processing flow applied to WM and TM seismic profiles is presented as supplementary material.

Diagnostics criteria used for identifying contourites based on seismic data were the ones proposed by Faugères et al. (1999), Nielsen et al. (2008), Camerlenghi and Rebesco (2008), and Rebesco et al. (2014). We used the definition of ‘‘Contourite Depositional System’’ (CDS), as an association of various drifts and related erosional features deposited in different times by different water masses as proposed by Hernández-Molina et al. (2008).

In the study area, we distinguished twoworking areas, named western and eastern sectors, based on water depth range, coverage by seismic reflection profiles and location of contourite drifts (Fig. 1b). The western sector is the deepest one, being located from about 4350 m to below 4800 m water depth, being crossed by profiles WM-02 and WM-03 (Fig. 1b). The eastern sector is shallower, from about 3000 to 4200 m water depth and it is covered by the profiles TM-60 and TM-64 (Fig. 1b).

5. Results

5.1 Seismic stratigraphy

Seismic stratigraphic interpretation allowed identify six seismic units (U1 to U6) and a sub-unit (U6a) separated by discontinuities (D1 to D6) and described as follows. They were correlated between the western and eastern sectors based on the similarities of their main seismic facies (Fig. 4) to overcame the absence of crossing profiles in the study area.

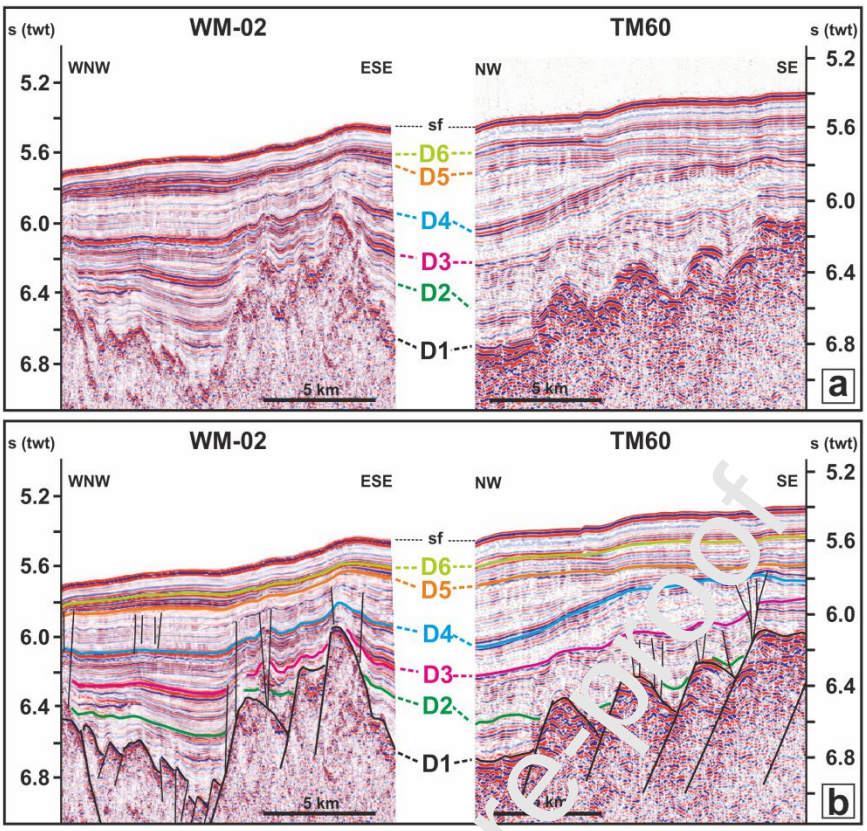

Figure 4 – Proposed seismostratigraphic correlation between discontinuities identified in seismic profiles WM-02 and TM-60 based on the similarity of seismic facies. D1 – Top of acoustic basement (ocean crust); D2-D6 – Discontinuities; sf- seafloor.

Acoustic basement

The acoustic basement consists of a succession of fault-blocks bounded by normal faults dipping toward WNW to NW and ESE to SE, defining either half-grabens or areas of large horsts (Figs. 5 to 8). Acoustically, the basement is topped by a high amplitude and discontinuous reflection (discontinuity D1) defining a rough and irregular surface offset by faults (Figs. 6 to 9). The basement deepens gradually from east to west. In the western sector, its top is in general located at below 6.8-7.0 s twt below seafloor (Figs. 5, 6) while in the eastern sector ranges from 4.2 to 5.7 s twt (Figs. 7, 8). This general trend is interrupted locally by the presence of several buried structural highs with summits placed at shallower sub-bottom depths, some of which at only 0.2 s twt beneath the sea floor (Fig. 5). On the other hand, basement's top can reach sub-bottom depths of around 7.2 to 7.4 s twt in half-grabens. Acoustic basement's internal seismic facies change from high amplitude, parallel, irregular and discontinuous reflections near its top to either chaotic or

semitransparent downwards. In the eastern sector, high amplitude, good continuity and closely spaced parallel reflections are observed within the basement dipping toward NW (Fig. 7). These intra-basement reflections are absent in the western sector.

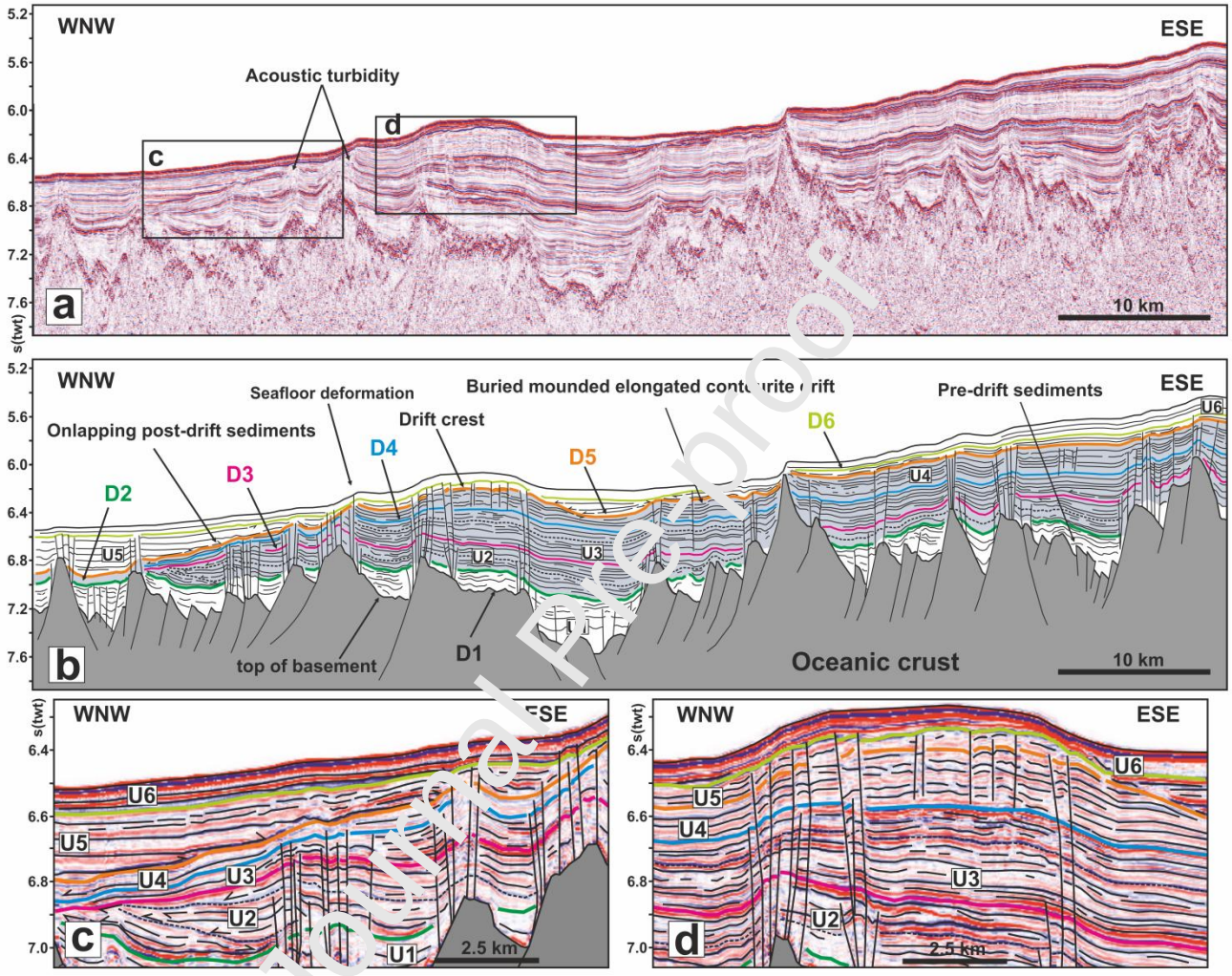

Figure 5 – a) Multichannel seismic reflection profile WM-02 (see Figure 1b for location). b) Line drawing interpretation, indicating the main discontinuities (D1-D6) and seismic units (U1-U6). Seismic units U2 to U4 form a mounded and lenticular shape body with pinch-out terminations toward west and interpreted as a buried giant, elongated and mounded contourite drift c) Detail of line drawing interpretations in the westernmost part of the drift where internal reflections of seismic units U5 onlap discontinuity D5 (orange) testifing the drift inactivity. Unit U6 drapes over U5 and covers uniformly the mounded drift preserving its shape. The sediments are cut by several sets of faults, some of them rooted on the oceanic crust. They disrupt units U1 to U5 and are sealed by discontinuity D6 (olive green). d) Detail of line drawing interpretation

in the drift crest zone showing its mounded geometry and lenticular shape of seismic units. Black dashed lines represent discontinuous or fainted reflections. Locally, reflections terminate against them.

Seismic unit U1

Unit U1 covers directly the basement, draping over discontinuity D1, mimicking the underlying topography. In the western sector, seismic facies near its base is either semi-transparent or stratified with parallel, low amplitude and very discontinuous reflections, evolving upwards to stratified facies with alternating low and high amplitude continuous reflections. This unit can reach ~0.5 s twt in sedimentary thickness and shows aggradational configuration, filling the basement grabens and onlapping their walls. In the eastern sector, seismic facies and thickness are similar, although thins (to <0.05 s twt) toward east on top of the large WNW-tilted basement block (Fig. 8). There, unit U1 is almost inexistent, being deeply truncated by the high amplitude discontinuity D2 (Figs. 7, 8). In both sectors, unit U1 is locally deformed by faulting showing chaotic facies with low amplitude and discontinuous reflections (Figs. 7, 8).

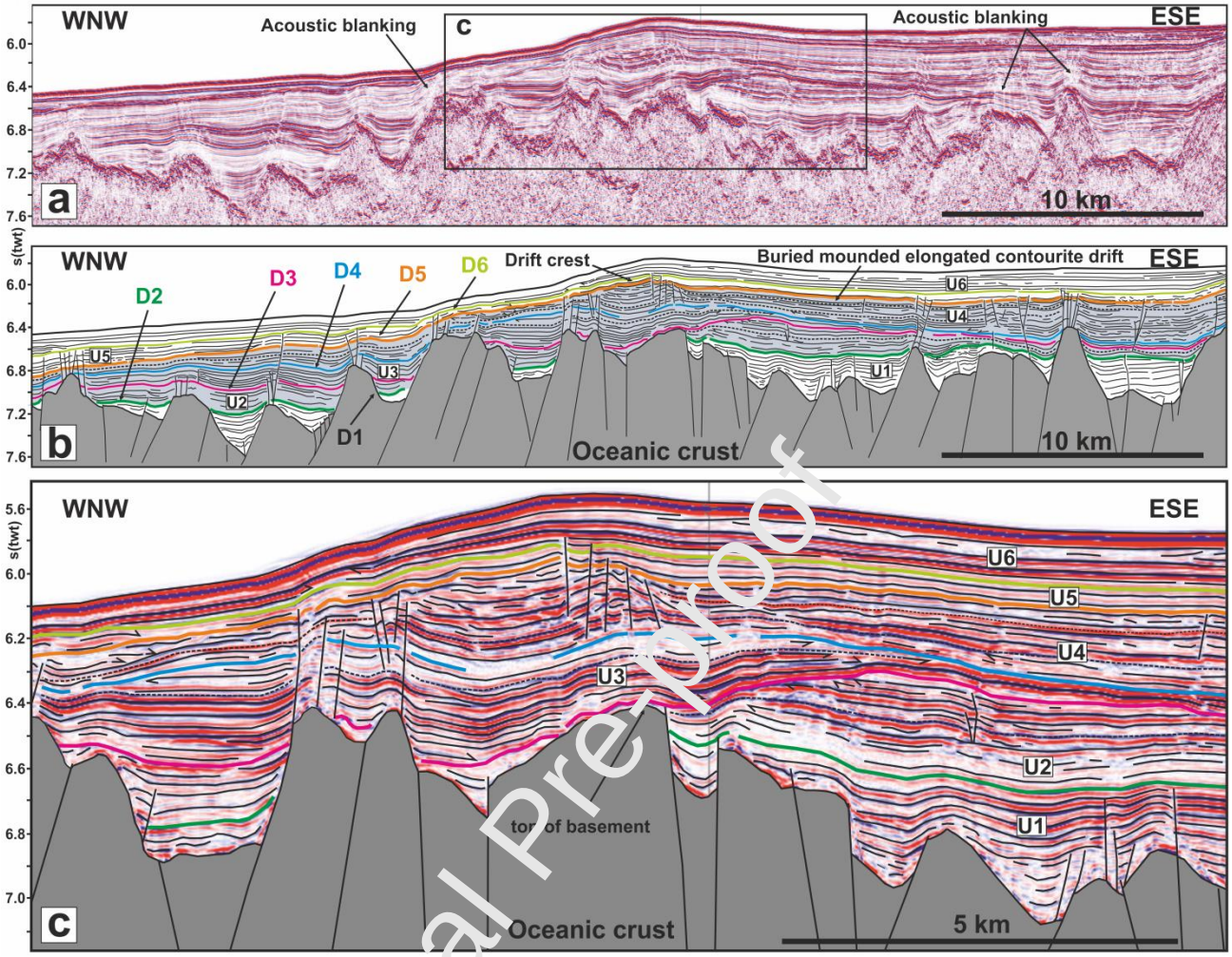

Figure 6 – a) Multichannel seismic reflection profile WM-03 (see Figure 1b for location). b) Line drawing interpretation, including the main discontinuities (D1-D6) and seismic units (U1-U6).The mounded and lenticular shape body is interpreted as a buried giant, elongated and mounded contourite drift onlapped by the overlying reflections of unit U5. c) Detail of line drawing interpretation in the drift crest zone showing several erosional truncations between discontinuities D3 and D5. Black dashed lines represent discontinuous or fainted reflections. Locally, reflections terminate against them.

Seismic unit U2

This unit lies on discontinuity D2 and its seismic facies and configuration changes laterally from west to east. In the western sector, seismic facies is semi-transparent with fainted reflections near the base changing toward the top to stratified facies with alternating parallel, very continuous, high and low amplitude reflections (Fig. 5). Internal reflections terminate in downlap against discontinuity D2 and are truncated at top by discontinuity D3. The configuration of seismic unit U2 is overall aggradational but its geometry changes from sheeted at east to lenticular asymmetrical with pinching out terminations over D2 toward west (Fig. 5). This change is accompanied by a reduction

in the sedimentary thickness from 0.3 s to <0.05 s twt in the same direction. Towards north and, D3 truncates locally U2 near the top of some fault-blocks reducing abruptly its thickness to less than 0.05 s twt (Fig. 6). In the eastern sector, U2 varies from semi-transparent with few discontinuous and fainted reflections (Fig. 7) to stratified with parallel and continuous reflections that grades to semi-transparent to the top (Fig. 8). Internal reflections are either concordant with D2 or onlap it toward east. Seismic unit U2 exhibits a slight mounded and elongated configuration and become thinner over the Madeira plateau reaching less than 0.05 s thickness. There, it is deeply truncated by D3 and the upper stratified and semi-transparent facies are absent (Figs. 7, 8).

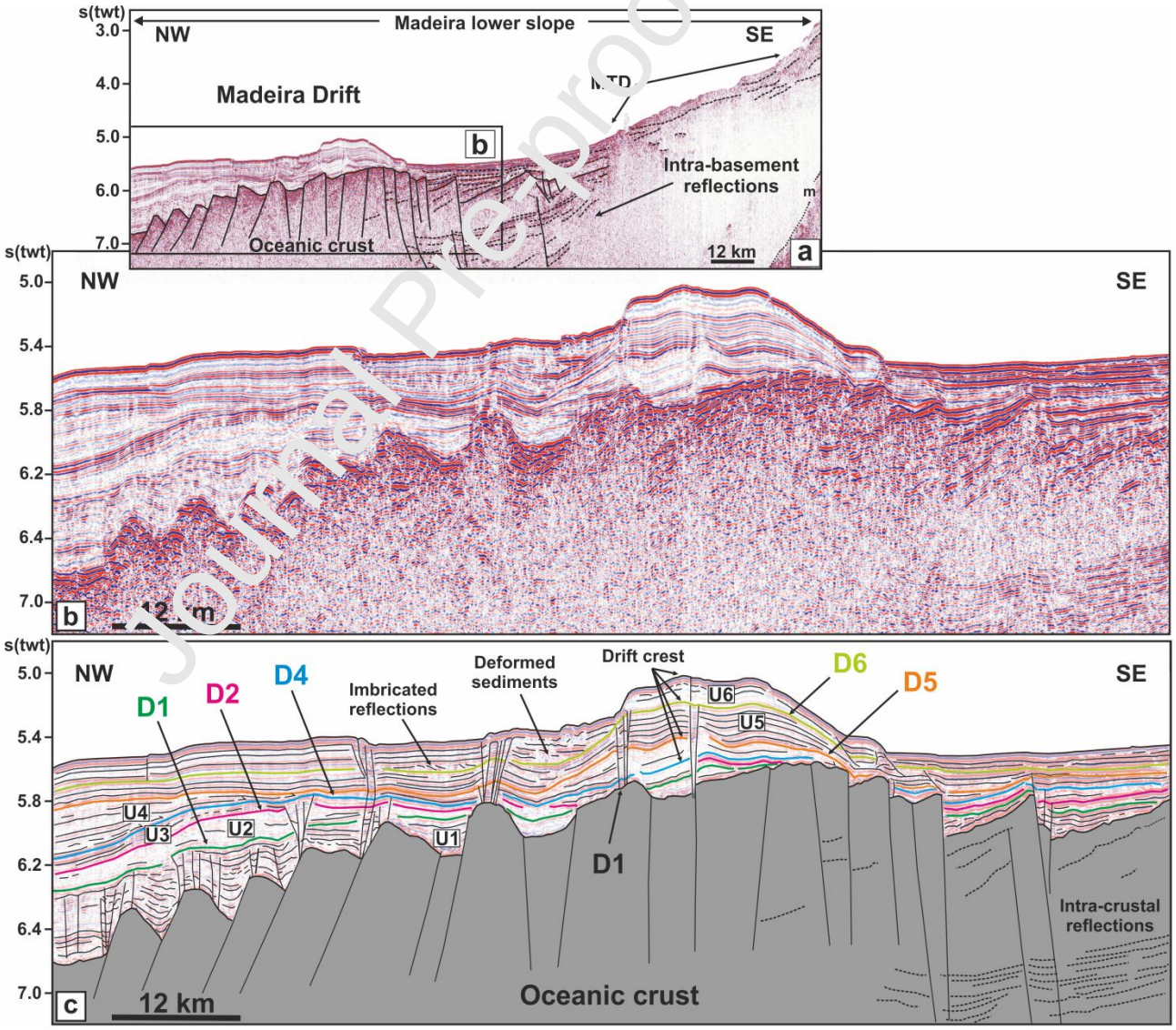

Figure 7 – a) Multichannel seismic reflection profile TM-60 showing the Madeira Drift developed on the lower slope of Madeira Island (see Figure 1b for location). Mass transport deposits (MTD) are also seen on the slope toward SE. b) Detail of seismic profile TM-60. c) Line drawing interpretation including the main discontinuities (D1-D6) and seismic units (U1-U6).

Seismic unit U3

Unit U3 rests unconformably over discontinuity D3 and shows different seismic facies and configuration in the western and eastern sectors. It is truncated in both sectors by discontinuity D4, an irregular, good continuity and medium to high amplitude reflection (Figs. 5 to 8). In the western sector, the configuration of U3 is similar to unit U2, changing from aggradational and conformable at east to wedge-shaped toward west showing pinch-out terminations and downlap reflections (Fig. 5). Thickness ranges from 0.25 s twt at east and <0.05 s twt at west. But toward north, the configuration of U3 varies to lenticular asymmetrical with a central mounded geometry (~0.3 s twt thick) that thins laterally in both sides, reaching the minimum sedimentary thickness of <0.05 s twt (Fig.6). Internally, U3 consists of a set of parallel reflections with high amplitude and good continuity alternating with lower amplitude reflections, and thus defining stratified seismic facies. In the eastern sector, the configuration and seismic facies of unit U3 are distinct from south to north. At south, U3 presents a slight mounded configuration thinning toward east as it is profoundly truncated by D4 and reach <0.01 s twt (Fig. 8). Seismic facies is semitransparent with discontinuous and fainted reflections. Toward northeast, unit U3 seems to be more aggradational with stratified facies that changes to semitransparent towards the Madeira plateau (Fig. 7). Its thickness has a decrease in the same direction reaching <0.01 s twt.

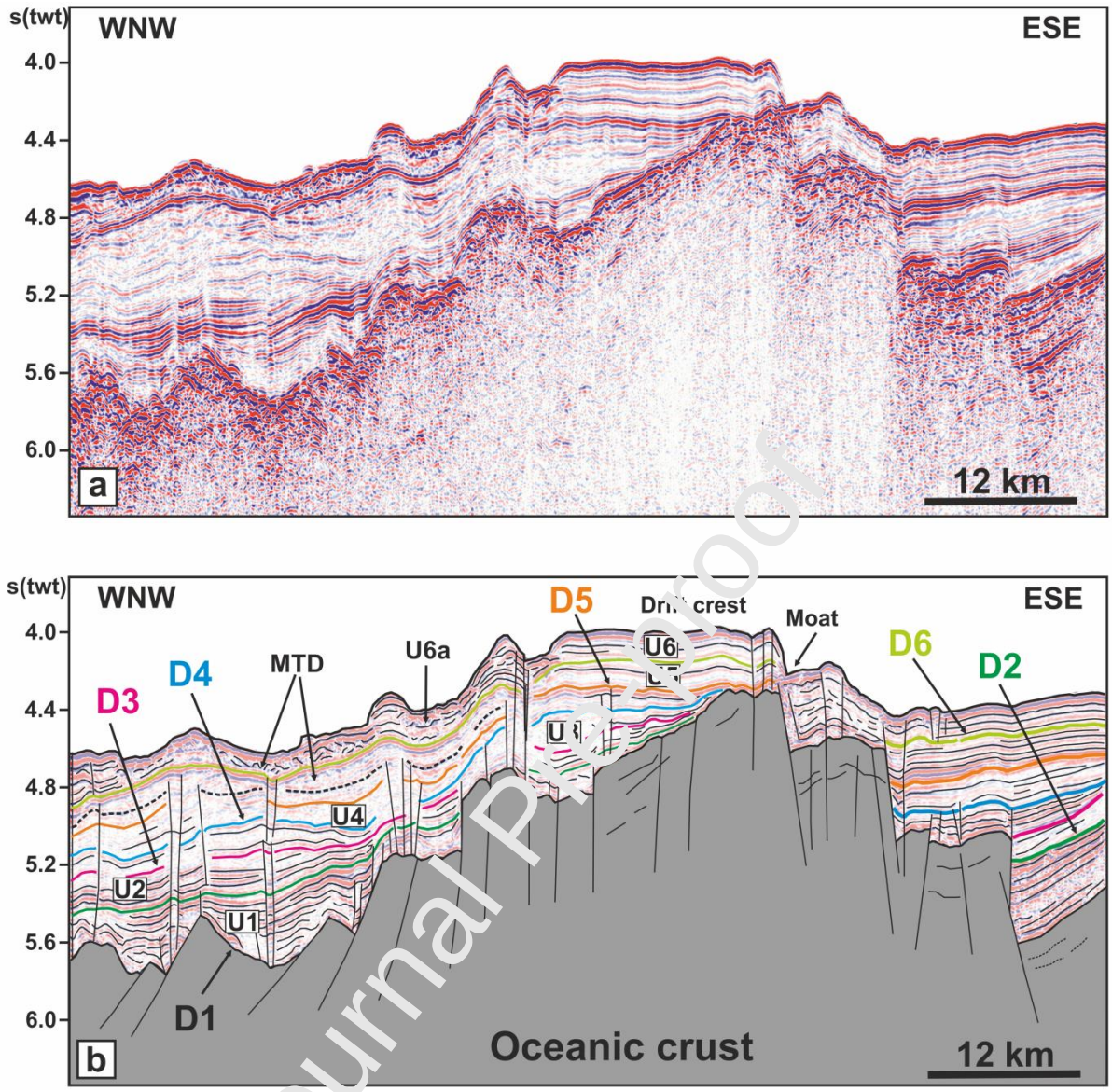

Figure 8 – *a)* Multichannel seismic profile TM-64 (see Figure 1b for location). b) Line drawing interpretation, including the main discontinuities (D1-D5) and seismic units (U1-U6). Note the presence of sub-unit U6a identified only in this seismic profile. MTD: mass transport deposits.

Seismic unit U4

In southern part of the western sector, U4 kept the lenticular asymmetrical shape of unit U3 although showing an important decrease of its thickness toward west (Fig. 5). Toward north, it is more mounded grading to sheeted in the Madeira plateau direction. The thickness increases in this direction reaching about 0.4 s twt (Fig. 6). The seismic facies varies from stratified to semitransparent as described for the previous seismic units. Unit U4 is truncated by discontinuity D5, which is a high amplitude and high continuity reflection. This truncation is more evident at west

because D5 passes gradually to conformable toward east (Figs. 5, 6). In the eastern sector, unit U4 also preserved the configuration of the previous units (Fig.8) although showing a mounded shape in the deeper part (Fig. 7). Internal reflections downlap either discontinuity D4 or the basement (Figs. 7, 8). Acoustic facies changes from semitransparent with discontinuous reflection to parallel, well-stratified, with alternating low and high amplitude and very continuous reflections. The sedimentary thickness of U4 in the eastern sector ranges from ~0.08 to 0.50 s twt.

Seismic unit U5

Unit U5 represents a major change in configuration observed in both sectors. In the western sector, U5 presents an aggradational sheeted geometry and internal reflections successively onlap D5 toward east or drapes over the underlying unit U4 (Fig. 6). Seismic facies are stratified with parallel, low continuity reflections, alternating between low and medium amplitude. The sedimentary thickness varies between 0.35 s and 0.08 s twt (Figs. 5, 6). The aggradational geometry continues to be dominant in the eastern sector (Fig. 8), although a mounded geometry developed on top of a basement high towards north (Fig. 7). Seismic facies is stratified, formed by parallel reflections with alternating low and high amplitude. Usually, they show good continuity. The sedimentary thickness ranges between 0.2 and 0.3 s twt (Figs. 7, 8).

Seismic unit U6

Unit U6 is bounded at base by discontinuity D6 and at top by the seafloor reflection. Discontinuity D6 is, as the previous ones, characterized by high continuity and high amplitude. Unit U6 presents homogeneous stratified seismic facies in both sectors, being characterized by parallel high-amplitude reflections in the lower part and semi-transparent to low amplitude reflections in the upper part (Figs. 5, 6, 7). The sedimentary thickness ranges from about 0.20-0.30 s twt (Figs. 6, 7, 8) to <0.05 s twt (Fig. 5). In the western sector, unit U6 displays a sheeted geometry with a clear aggradational component (Figs. 5, 6) that drapes over U5. In the eastern sector, its geometry changes from south to north. A tabular shape is observed at south, showing parallel and

conformable reflections and defining an almost flat topography bounded by symmetrical steep flanks (Fig. 8). At northeast, the shape of U6 is mounded with downlap terminations over D6 and forms a convex and asymmetrical topography on the seafloor (Fig. 7). Thickness is almost constant, around 0.2 s twt. This unit is bounded at east by an asymmetrical depression with a steeper western wall that range from ~3150 m (at south) to ~3900 m (at north) water depth (Figs. 7, 8).

Seismic sub-unit U6a

Sub-unit U6a is only recognized in seismic profile TM-64 (Fig. 8). It is a dominantly chaotic seismic sub-unit that only outcrops in the southern part of the eastern sector between ~3000 and 3450 m water depth (Fig. 8). It corresponds to a tabular-shape body with almost constant sedimentary thickness of 0.18-0.20 s twt, which produces a rough and irregular seafloor topography. Although chaotic facies prevail, semitransparent and layered facies can be observed locally. Elevated mounded blocks with parallel fainted internal reflections are presenton top of U6a (Fig. 8). Sub-unit U6a is underlain by an irregular, high amplitude and high continuity reflection dipping toward west that seems to be correlative of D6 (Fig. 8). In the northern part of eastern sector, below 4400 m water depth, minor buried lens-shaped of chaotic or imbricated facies occurred close to the base of U6 (Fig. 7).

5.2 Sediment faulting

Faulting of the seismic units is a pervasive phenomenon in the study area, affecting the entire sedimentary column of western and eastern sectors (Figs. 5 to 8). Several sets of extensional faults cut through the sediments and two types can be distinguished taking in account their geometry and stratigraphic position. The most abundant correspond to sets of near-vertical, closely spaced faults rooted in the basement blocks. Some of these sets are circumscribed to seismic unit U1 (Fig. 7a) while others cut through younger sediments being sealed either by discontinuity D4 or D6. A few faults affect the upper sediments of unit U6 and deform the seafloor (Fig. 6). Acoustic turbidity is

sometimes associated with these faults. The other type of faults, in minor number and more localized, consists of a set of vertical, parallel, and equally spaced faults developed within a specific stratigraphic interval. They occur mostly within unit U4 and are rooted in a layer above discontinuity D4 and usually sealed by discontinuity D5, although in some places the seal is the discontinuity D6. The occurrence of this type of faults is concentrated in the central part of unit U4 in the western sector (Figs. 5, 6).

6. Discussion

6.1 Nature of acoustic basement

The fault-blocks structure and seismic attributes shown by the acoustic basement in the study area are the ones typical of the layer 2 of oceanic crust generated in a Cretaceousspreading center (Searle et al., 1985). Its precise age is undetermined because it is located within the CMQZ, *i.e.,* between Chrons M0 (~120 Ma) and C34 (83.5 Ma) (Bird et al., 2007) (Fig. 1a). Bearing in mind this limitation, we attempted to better constrain its age considering that i) the age of tholeiitic basalts drilled at DSDP Sites 136 and 137 (Hayes et al., 1972) is early Aptian and late Albian, respectively, and ii) the age of oceanic crust located eastward from 30ºN 23ºW should be older than 106 Ma according to Searle et al. (1985). Therefore, we propose that the oceanic crust in the study area is at least Aptian and no younger than Late Albian (Fig. 1, 5). Usually, oceanic crust older than 80-100 Ma is located below 5500 m water depth (Crosby et al., 2006; Wang et al., 2011), but in the eastern sector of the study area near the Madeira plateau it is shallower than expected for an Early Cretaceous oceanic crust. There, the top of the oceanic crust deepens from east to west, in clear contrast to what is supposed to happen in an old crust. This indicates that other mechanism besides thermal subsidence as it moved away from the Cretaceous spreading center should account for its present depth. Residual basement topography shows a positive anomaly around Madeira archipelago, derived from thermal uplift associated with mantle plume activity (Crosby et al., 2006; Wang et al., 2011). While both thermal uplift and magmatic intrusions affected the oceanic lithosphere underlying present-day Madeira Island, the surrounding seafloor was

unaffected by magmatism but suffered deformation by uplift and tilting of large segments of oceanic lithosphere (Fig. 6, 7). This process can explain the odd depths shown by the oceanic crust in the eastern sector, located closer to the Madeira archipelago. The uplift created a broad elevated relief with steep slopes, corresponding to a westward tilted segment of oceanic crust fault-blocks capped by sediments of seismic unit U1. On the other hand, the continuation of thermal plume piercing over time conducted to several pulses of magmatic activity leading to emergence of Madeira Island in the late Miocene (Ramalho et al., 2015). The set of parallel, high amplitude reflection observed within the oceanic crust in the eastern sector can be interpreted as sills intruded during these magmatic phases (Fig. 7). It is unknown when the thermal uplift started, but the Madeira submarine volcanic plateau began to grow near the Paleocene-Eocene boundary at about 60 Ma (Schmincke, 1982; Hoernle et al., 1995). Nevertheless, earlier submarine volcanism episodes might have occurred as recorded by the ~88.5-65.0 Ma volcanic tuffs found at DSDP Site 136 (Hayes et al., 1972) (Fig. 3) and by a magnetization axis of Early Cretaceous age identified in the Madeira plateau (Abranches et al., 1984).

6.2 Type of deposits and their sedimentary stacking patterns

6.2.1 Pelagic deposits

The oldest deposits correspond to seismic unit U1 that draped over the underlying Early Cretaceous oceanic crust, filling partially the half-grabens and smoothing its topography. The aggradational stacking pattern and prevalence of semi-transparent to stratified seismic facies across the study area indicates the persistence of almost uniform depositional conditions for a long-time and predominance of fine-grained sediments deposition (Shipley et al., 1983). Usually, the stratified facies' type reflects successive changes in acoustic impedance related to lithological variations (Figs. 5,6). It commonly corresponds either to distal fine-grained turbidite deposits or carbonate oozes interbedded with pelagic clays (Hüneke and Henrich, 2011). Thus, considering the absence of evidences (e.g., channels and levees) for turbidity features the influence of turbidity

currents isdiscarded , but the dominant draping geometry, suggest a dominant pelagic deposition by vertical settling in a low hydrodynamic deep-water environment. .

6.2.2 Contourite drifts and bounding discontinuities

The seismic facies and configuration displayed by seismic units U2 to U6 allowed interpreting them as contourite drift deposits, separated by the erosional surfaces D2 to D6.Overall, the seismic units form giant elongate and mounded contourite successions based on the Rebesco et al. (2014) classifications. Among the erosional surfaces, discontinuities D2 and D5 mark the most profound changes in the depositional environment evidenced by strong erosion and abrupts changes in the depositional stacking pattern of overlying seismic units. Discontinuities D3, D4 and D6 also exhibit an erosional character but less pronounced compared with D2 and D5 and the configuration of seismic units that they bound is more or less maintained. The discontinuity D2 incises deeply the underlying pelagic sediments of unit U1 and represents the oldest erosional event identified in the study area. Therefore, D2 testifies an important event, probably linked to the initiation of significant and a persistent deepwater circulation in this sector of the NE Central Atlantic. Usually, strong erosional events preceded contourite deposition, being recorded as high amplitude and continuity reflections (e.g., Faugères et al., 1999). D2 is overlain by the first contourite drift deposits (unit U2) that start to accumulate as the bottom current slowed down. The next younger major modification in the deepwater mass circulation is reported by discontinuity D5, which truncates the underlying seismic units. In the deeper western sector, this erosional surface is onlapped towards east by reflections of unit U5. Hence, discontinuities D2 and D5 are recording the two main changes in the paleocirculation, which lead to the edification of two distinct contourite depositional systems designated as CDS-1 (units U2, U3 and U4) and CDS-2 (units U5 and U6).

CDS-1

The geometry and characteristics display by deposits from seismic units U2 to U4 allowed define the elongated and mounded contourite Drift 1 that characterizes the CDS-1. In synthesis they arei)

an up-ward convex shape and asymmetrical geometry, ii)units downlap or drape onto previous deposits, iii) show a general lenticular geometry that thins laterally, in particular toward the Madeira plateau, iv) while laterally U2 and U4 are cut by several truncations laterally, their central parts are thicker showing a clear aggradational geometry. The shape and geometry of Drift 1 is similar to other giant elongated and mounded drifts found in the Atlantic, such as Blake Bahama Outer Ridge, Greater Antilles Outer Ridge, Bermuda Rise, Eirik Drift (Hunter et al., 2007), Agulhas Drift, (Niemi et al., 2000), and in the Argentina margin (Hernández-Molina et al., 2010). The extension and great thickness reached by Drift 1 indicate a long term influence for the deepwater mass conditions in the study area. The end of Drift-1 is recorded in the western sector by its progressive covering by sediments of unit U5 onlapping discontinuity D5, but conserving the original morphology of Drift 1. Thus, it can be considered as a buried drift, recording the occurrence of a major change in paleoceanography and depositional conditions that led to its inactivity. The sedimentary stacking pattern of contourite drifts has been widely used to deduce changes in paleocurrents pathways and intensity (e.g., Fauguères et al., 1999; Rebesco and Camerlenghi, 2008; Gruetzner and Uenzelmann-Neben, 2016). Considering that Coriolis Effect on Northern Hemisphere impose rightward downcurrent erosion (e.g., Faugères et al., 1999), drifts develop laterally to the respective main core of the bottom current. Therefore, the morphology displayed by Drift 1 indicates that it was built-up by a long-term northwards flowing bottom current, forced to diverted to the right in the Northern Hemisphere due to the Coriolis Effect.

CDS-2

Deposits from seismic units U5 and U6 define Drift 2, which characterize the CDS2, present an asymmetrical, slight mounded shape and dominant aggradational geometry. Conversely to the buried Drift1, the Drift 2 forms a pronounced relief in the seafloor, which has been earlier recognized as an area swept by bottom currents (Heezen et al., 1959; Embley et al. 1978) and more recently as a giant contourite drift named Madeira Drift (Roque et al., 2015; 2022). The inactivity of Drift 1 was followed by the migration of contourite drift deposition eastward and the Drift

2 formation at shallower water depths on the Madeira plateau. Since contourite drift migration only occurs due to key oceanographic changes (Faugères et al., 1999; Hernández-Molina et al., 2009), this migration testifies a major modification in the deepwater circulation with lateral and vertical shift of the water masses. The shape of Drift 2 changes from north to south. At north, Drift 2 shows mounded-shape with aggradational geometry (Fig. 7). At south, it displays a sheeted-shape with almost flat top, steep flanks and also aggradational geometry (Fig. 8). This shape results from the incision of a moat at the foot of the eastern flank and disruption of its western flank by slope failure. While a well-defined an asymmetrical moat developed at the south (3150 m water depth), at the north only a broad and wider depression exists reaching 3900 m water depth (Fig. 7). The crest of Drift 2 shallows from north to south. It is located at ~3750m in water depth, at north and at ~3000m water depth, at south. The overall shape and sedimentary stacking pattern shown by Drift 2 allowed classifying it as an elongated, mounded and separated drift based on the Rebesco et al. (2014) classifications. The morphology of Drift 2 morphology and its moat location at east indicate that it has also been built-up by a persistent and stable northward flowing bottom current. It , has also been diverted to the right by the Coriolis Effect as Drift 1.

6.2.3 Mass transport deposits

In the study area, the presence of chaotic seismic facies is restricted to the shallower eastern sector and corresponds to seismic sub-unit U6a (Fig. 8) and in minor extent to localized, small and buried chaotic bodies within U5. Considering its seismic and morphological characteristics, we interpreted it as mass transport deposits (MTD) resulting from upslope disruption of previous unit U6 and U5. The discontinuity D6 that underlies this chaotic body can correspond to the basal shear plan of the MTD.. The buried MTDs recognized interbedded within contourite sediments of seismic unit U5 indicate recurrent, but smaller, episodes of slope-failure (Fig. 7). The outcropping MTD (U6a) in the western flank of Drift 2 was firstly recognized and described by Embley et al. (1978). These authors referred the presence of a field of hyperbolic echoes and interpreted them as a large slide. Typical features resulting from interaction between bottom-currents and slide scars as infill

drifts are seemingly missing. This absence seems to corroborate the relict condition for the CDS-2 as early proposed by Embley et al. (1978).

6.3 Age framework

The precise age of discontinuities and seismic units identified in the study area is unknown because there is no direct stratigraphic control available. To overcome this, we propose a theoretical age for them taking in consideration the following constraints: i) the age of sediments and unconformities/hiatuses recognized in DSDP and ODP drills made near Madeira Island and along the NW African margin (Hayes et al., 1972; Lancelot et al., 1978; Ruddiman et al., 1988; Schmincke et al., 1995) (Fig. 9), ii) the interpretation by previous authors that these unconformities/hiatuses result from intensification of bottom currents activity and pinpoint strengthening periods at regional scale (e.g., Tucholke and McCoy, 1986; Mountain and Miller, 1992; Mourlot et al., 2018), iii) the configuration of Drift 1 and Drift 2 indicate that they were deposited by a northward flowing water mass suggesting a southern source for it, and iv) the Atlantic deep-water circulation changes referred in the literature. The theoretical age proposed for the seismic units and discontinuities identified is the following.

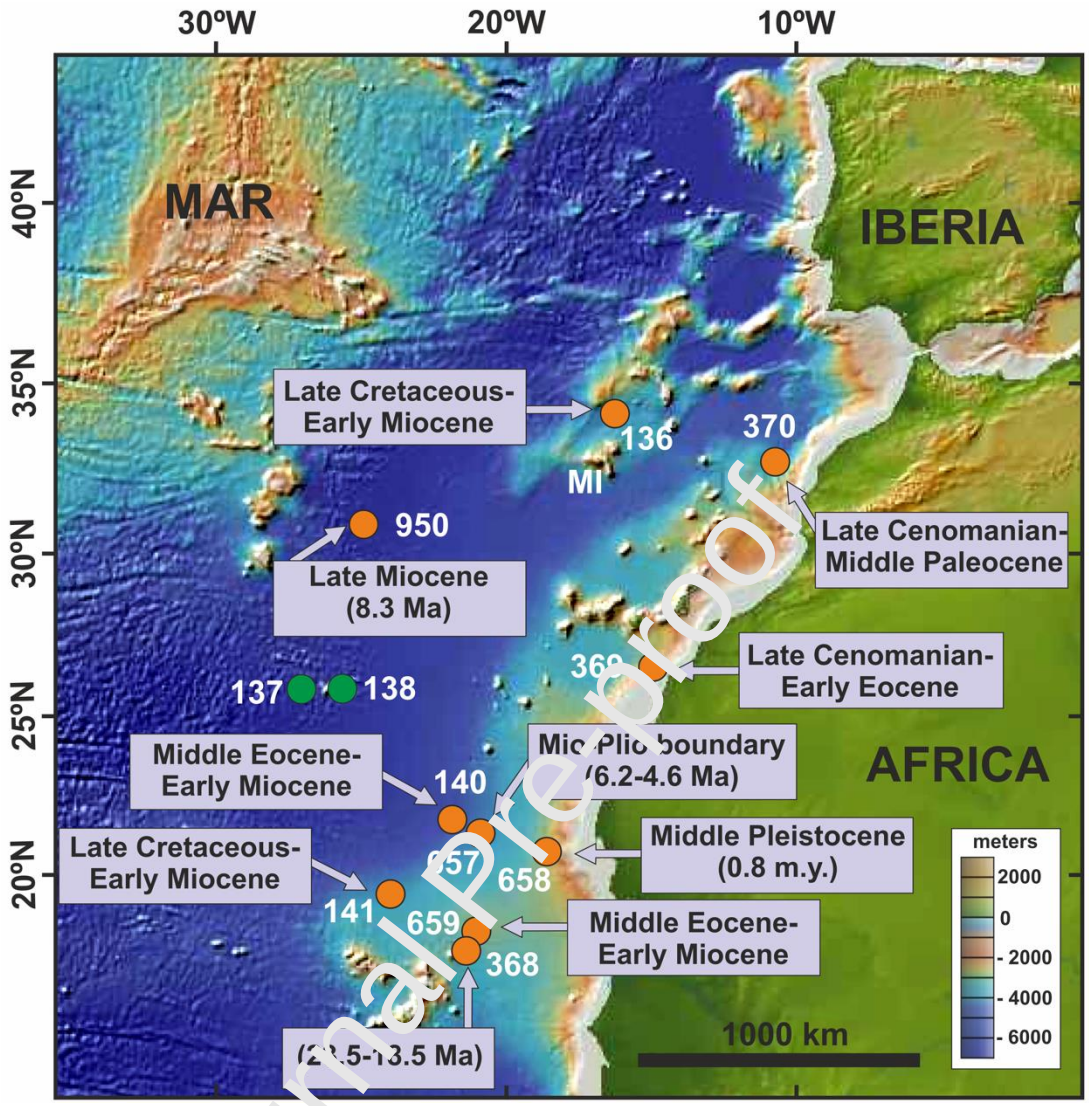

Figure 9 – Location of DSDP and ODP sites drilled along the Northwest African margin and adjacent deep basin (orange circles) and respective identified hiatuses (Hayes et al., 1972; Lancelot et al., 1978; Ruddiman et al., 1983; Schmincke et al., 1995). Sites 137 and 138 (green circles) are located in the deep basin and no hiatuses were found. Bathymetry from GeoMapApp (http://www.geomapapp.org).

Seismic unit U1 was tentatively correlated with pelagic sediments drilled at DSDP Site 136, namely, Aptian nannofossil ooze and calcareous muds, Late Aptian to Early Cenomanian banded colored clay, and Coniacian to Santonian silty clay with ash layers (Hayes et al., 1972). In the western sector located at depths >5200 m, seismic unit U1 can be also correlated with pelagites of Late Albian to Early Turonian retrieved at DSDP Site 137 (Fig. 9) corresponding to nannofossil marls, chalk ooze and clays (Hayes et al., 1972). Therefore, U1 spans from Aptian to at least Santonian.

Discontinuity D2 testifies an abrupt change in these depositional conditions putting an end to the dominance of pelagic sedimentation,recording the onset of a vigorous circulation of a northward deep-water mass. We correlated D2 with the hiatus documented at Site 136 (Fig. 1b, 3, 9), which has been attributed to erosion by strengthening of bottom currents circulation. There, sediments of latest Cretaceous (Campanian and Maastrichtian) and Paleogene are missing, suggesting thaterosion by bottom currents prevented significant deposition for 60 myr (Hayes et al., 1972; Lancelot et al., 1978; Ruddiman et al., 1988; Schmincke et al., 1995). Other prolonged hiatuses were found along the NW African margin (Fig. 9), which spanned from the latest Cretaceous to the majority of Paleogene (Sites 369, 370) and early Miocene (Site 368). In fact, multiproxy evidence indicates deep-water circulation in the Central and North Atlantic since Campanian-Maastrichtian times, involving the flowing of the SCW sourced in the Southern Ocean (e.g., MacLeod et al., 2011; Friedrich et al., 2012; Murphy and Thomas, 2013; Sabatino et al., 2018; Ladant et al., 2020; Palcu et al., 2020). A similar age hiatus, separating sediments of Early to Late Cretaceous age from overlying Early Miocene hemipelagic clays was discovered in the Western North Atlantic and was also interpreted as derived from bottom currents erosion (Hollister and Heezen, 1972; Tucholke and Vogt, 1979).Therefore, we propose that discontinuity D2 formed in latest Cretaceous (Campanian-Maastrichtian) up to the beginning of Paleocene due to the northwards circulation of the SCW. It testifies the clear first incursion of the SCW in this sector of the NE-Central Atlantic. Consequently, the oldest deposits of unit U2 started to accumulate near this timeframe.

Discontinuities D3 and *D4* are of uncertain age because all the Paleogene or part of it is absent at the majority of the DSDP drilled sites, *i.e.* sites 136, 140, 141, 368 and 368 (Fig. 9). Both discontinuities deeply truncate the underlying seismic units U3 and U4, recording erosional episodes interpreted as being linked to the enhancement of bottom current circulation before the deposition of these units. In fact, a widespread hiatus spanning most of the Paleocene has been identified worldwide (Spencer-Cervato, 1998). Moreover, a Late Paleocene (~60 Ma) widespread seafloor erosional event has been recognized in several sites of the Atlantic (Mountain and Milles, 1992). There is also evidence from stable isotopes that the SCW was able to penetrate in the North

Atlantic as far as the Bay of Biscay in the Paleocene and Eocene (Pak and Miller, 1992). The enhancement of SCW circulation in the middle Eocene and near the Eocene-Oligocene transition is well known (e.g., Zachos et al., 2001; Sher and Martin, 2006). Furthermore, Dutkiewicz and Müller (2022) recognized a period of important carbonate dissolution in the mid-Eocene at about 44-38 Ma. It seems that a more corrosive water masse circulated at that time in the Central Atlantic. Although carbonate dissolution can produce important hiatuses in the sedimentary record it remains unknown the role of this process in the formation of discontinuities in the study area. The seismic characteristics shown by discontinuities D2 to D6 indicate a clear erosional origin, and no linked to carbonate dissolution can be drawn based only on seismic reflection data.

Thereby, based on these known global paleoceanographic changes we propose that D3 and D4 formed by seafloor erosion during the Paleogene. Thus, we speculate that unit U3 might have developed near the Eocene-Oligocene transition.

Discontinuity D5 represents the second main change in depositional conditions in the study area with the eastwards migration of contourite deposition to shallower water depths. Discontinuity D5 can be correlated with the absence of early Miocene sediments at Sites 140, 141 (Hayes et al., 1972) and 368 (Lancelot et al., 1978) and with the ~23.5-18.5 Ma hiatus found at Site 659 (Ruddiman et al., 1988). In fact, widespread early Miocene unconformities and hiatuses have been found in Atlantic deep-sea sediments (Flower et al., 1997; Spencer-Cervato, 1998) while a middle Miocene (~15 Ma) hiatus has been identified in the Southern Ocean (Wright and Miller, 1993; Tagliaro et al., 2021). Both hiatuses have been related to the strengthening of the AABW in the middle Miocene (e.g., Hall et al., 2003; Huang et al., 2017), coinciding with significant ice sheet expansion on Antarctica (Miller et al., 2005). Dutkiewicz and Müller (2022) also identified a period of increased carbonate dissolution in the Mid-Late Miocene ~19-8 Ma affecting the Central Atlantic. However, is uncertain the role of this process in the origin of discontinuity D5. As discontinuities D3 and D4, D5 also shows a clear erosional character. Therefore, we suggest that D5 could testify the middle Miocene enhancement of the AABW. The overlaying seismic unit U5 might have started to

be deposited in the middle Miocene, marking the onset of Drift 2 accumulation in the eastern sector.

Discontinuity D6 marks the base of the youngest seismic unit U6 and represents other erosional event of uncertain age. Considering that a major global cooling and pulse of increased formation of AABW occurred in Late Pliocene (e.g., Kleiven et al., 2002; Bartoli 2005; Mudelsee and Raymo, 2005; MaKay et al., 2012; Tagliaro et al., 2021), it seems likely that D6 could be related to these events. Regionally, the arrival of the corrosive AABW is testified by a carbonate dissolution hiatus near Late Miocene-Pliocene boundary found at Site 657 (Ruddiman et al., 1988). Considering both regional and global settings, we suggest that U6 might have accumulated from the Late Pliocene through the Quaternary. Since sub-unit U6a results from the disruption of this seismic unit, it will be at least of same age.

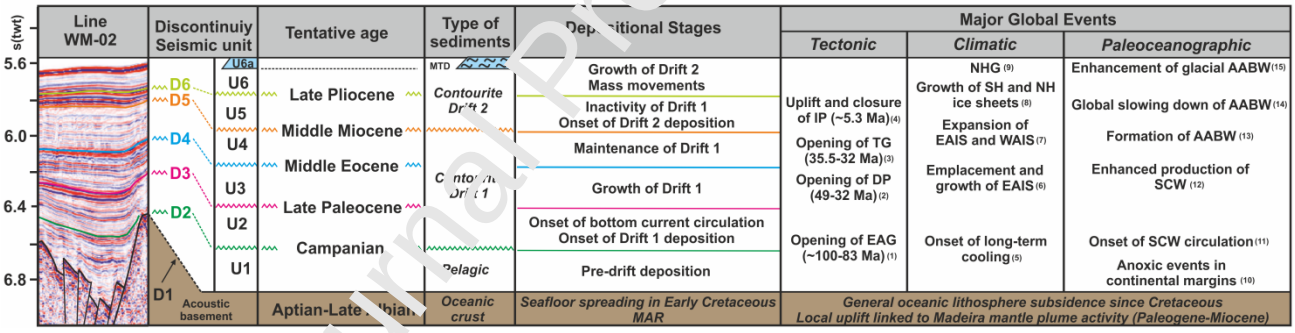

Figure 10 – Synthesis of discontinuities and seismic units identified in the study area presenting a tentative age for these discontinuities. The type of sediments based on the seismic characteristics is also given. The depositional stages proposed in this work and the main global events since the Cretaceous are also presented. The relationship between these discontinuities and DSDP and ODP sites shown in figure 9 is explained with detailed in section 6.3. EAG= Equatorial Atlantic Gateway: DP= Drake Passage; TG= Tasmanian Gateway; IP= Isthmus of Panama; EAIS= East Antarctica ice sheet; WAIS= West Antarctica ice sheet; SN= Southern Hemisphere; NH= Northern Hemisphere; NHG= Northern Hemisphere Glaciation; SCW= Southern Component Water; AABW= Antarctica Bottom Water; MAR= Mid-Atlantic Ridge. (1) Pérez-Díaz and Eagles (2017); (2) Lagabrielle et al. (2009); (3) Sher et al. (2015); (5) Huber et al. (2016); (6) Zhang et al. (2021); (7) Potter and Szatmari (2009); (8) Bartoli (2005); (9) Mudelsee and Raymo (2005); (10) Jenkyns (2010); (11) Palcu et al. (2020); (12) Toumoulin et al. (2020); (13) Hall et al. (2013); (14) Hassold et al. (2009); (15) Böhm et al. (2015).

6.4 Evolution of the Madeira Contourite Drift Systems and paleoceanographic implications

In synthesis, the sedimentary record of the study area has been build-up from the Early Cretaceous to the Quaternary by the activity of three main sedimentary processes, although with different degrees of importance: 1) pelagic settling, 2) deposition by bottom-currents and 3) mass movements. Among them, the second has been the long-lasted and dominant one. The other two sedimentary processes were only important during a restricted time interval as 1) or occur circumscribed to a specific area as 3). We propose a three stages depositional evolutionary model for the study area as follows (Fig. 10, 11). We also discuss the implications of the CDSs for a better comprehension of the deepwater circulation in the NE-Central Atlantic since the Late Cretaceous.

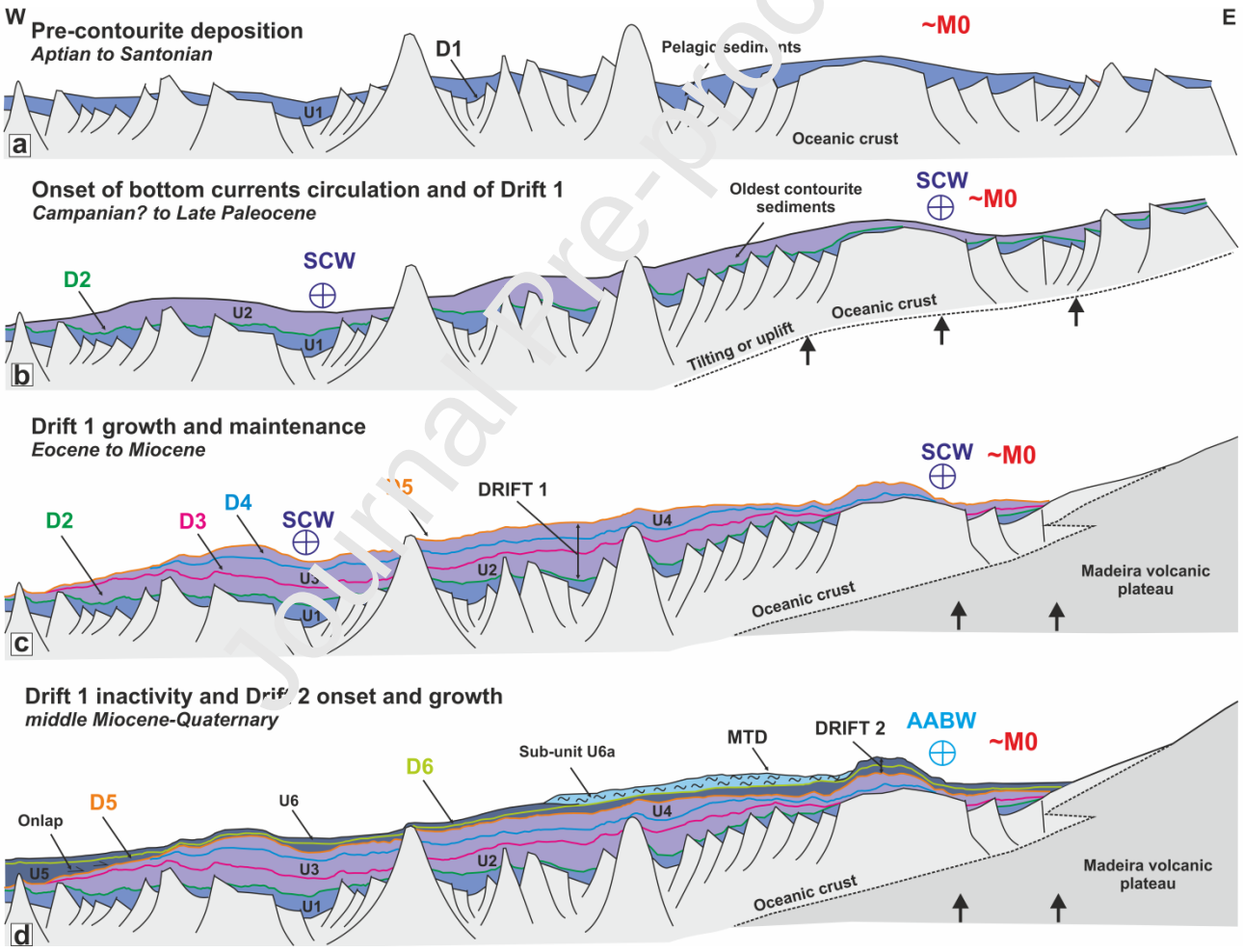

Figure 11- Sketch showing the main evolution depositional stages proposed for the study area. See text for details.

6.4.1 Stage I - Pre-contourite deposition (Aptian to Santonian?)

The pre-drift stage was dominated by deposition of pelagic sediments of seismic unit U1 above the top of oceanic basement (discontinuity D1). Thus, after the oceanic crust's formation in the Early Cretaceous Mid-Atlantic Ridge, Aptian carbonate oozes and muds draped over the fractured blocks filling the half-grabens. Afterwards, the oceanic crust spread away from the Mid-Atlantic Ridge, cooled and suffered thermal subsidence allowing the deposition of deeper banded and colored fossiliferous clays of Early Cenomanian age as the ones drilled at nearby Site 136 (Fig. 10, 11a). In the study area, bottom-currents started to be strong enough to rework the red clay sediments of Coniacian to Santonian age drilled at Site 136, producing parallel and cross laminations (Hayes et al., 1972). Regionally, bottom-currents already flowed along Guinea and Morocco margins in the Early Cretaceous (Dunlap et al., 2013; Mourlot et al., 2018).

6.4.2 Stage II – CDS-1: Onset, growth and maintenance (Campanian? to Early Miocene)

A SCWcoming from the south invaded the study area by Campanian-Maastrichtian times and its great erosional capacity produced discontinuity D2, truncating the underlying pelagic sediments of seismic unit U1 (Fig. 11b). Deposition resumed on the CDS-1 after this erosional event (seismic unit U2), reflecting a progressive reduction of the initial intensity of the bottom current from the end of the Cretaceous to the Late Paleocene (Fig. 11b). Several depositional features related to bottom current circulation during the Late Cretaceous have been recognized along the African margin. Dunlap et al. (2013) identified sediment waves of Late Cretaceous age offshore Morocco and Mourlot et al. (2018) recognized sediment waves and contourite drifts of the same age in the Senegal and Mauritania basins. According to these authors, the estimated paleo-depths of the contourite drifts range from 4150 to 4050 m. The deposition of these features at such paleo-depths reveals that the circulation of a deep-water mass along the NW African margin was already established in the Late Cretaceous. Furthermore, according to Tucholke and McCoy (1986), both Western and Eastern Central North Atlantic basins had already attained paleo-depths around 5000 m during Santonian times. Other Campanian-Maastrichtian age contourite drifts and associated

valleys, moats and channels formed by a NW-flowing water mass have been found along the NW Europe margin, namely, in the Danish Basin, Baltic Sea, southern England and NW France (Surlyk and Lykke-Andersen, 2007). In the Western North Atlantic, there is also deposition of contourite drifts during the Late Cretaceous-Paleocene interval. Contourite drift deposition on the eastern flank of the J-Anomaly Ridge started in the Campanian or early Maastrichtian and continued throughout the Paleocene (Tucholke and Ludwig, 1982; Berggren et al., 2000). In the Newfoundland Ridges, incipient contourite drifts developed from the Campanian-Maastrichtian to the Paleocene (e.g., Norris et al., 2014; Boyle et al., 2017). Other small and local drifts development in the Late Cretaceous-Eocene in the Flemish Cap, Chesapeake drift and in Nova Scotia margin (Campbell and Mosher, 2016; Rodrigues et al 2022).

By the Late Paleocene, the circulation between South and North Atlantic was fully established, and as a consequence we suggest that a pulse of SCW scoured discontinuity D3, which cuts deeply into underlying sediments of seismic unit U2. A prominent unconformity of Late Paleocene age (~60-57 Ma) has also been identified in the western Bermuda Rise (Tucholke and Voigt, 1979; Mountain and Miller, 1992). The existence of all these contourite drifts and erosional surfaces of similar age in opposite sides of the Atlantic demonstrates that important changes in deep-water circulation at ocean basin-scale occurred between the Campanian-Maastrichtian and the Late Paleocene, involving a southern sourced water mass.

The D3 erosional episode was followed by the accumulation and thickening of Drift 1 represented by seismic unit U3 (growth phase, ?Eocene to Oligocene), which kept the same lense-shaped configuration of U2 (Fig. 10, 11c). This indicates the stability and persistence of the northwards flowing SCW in this region of the Atlantic. This period of growth of Drift 1 is marked globally by the circulation of warm saline deep-water produced at multiple locations, including southern high latitudes, North Pacific and low latitudes regions (Ferreira et al., 2018). At that time, besides the circulation from the Southern Ocean through the South and Central Atlantic, low-latitude circulation was well established though the Central American Seaway and the Tethys Seaway, which connected the Pacific, Atlantic and Indian basins (Straume et al., 2020).

In addition to the SCW circulation, the accumulation of Drift 1 might have been favored by the bending and uplift of the oceanic lithosphere related to Madeira submarine volcanism, which started near the Paleocene-Eocene boundary at about ~60 Ma (Schmincke, 1982; Hoernle et al., 1995). The resulting topographic high should have acted as an obstacle to bottom-currents pathways and would have forced the SCW to contour it.

The stability of the environmental conditions that prevailed during deposition of U3 was interrupted by the strengthening of the bottom-currents and incision of discontinuity D4 possibly near the Eocene-Oligocene Transition (EOT). It is generally accepted that the formation and enhancement of a southern sourced water mass with similar characteristics as the AABW occurred at the EOT (e.g., Kennet, 1982; Goldner et al., 2014) following the beginning of Southern Ocean gateways opening in Late Eocene, as the Drake Passage (Lower and Gahagan, 2003; Diekmann et al., 2004; Miller et al., 2009; Straume et al., 2020). This time was marked globally by major changes in oceanic gateways such as deepening of the Greenland-Scotland Ridge and shallowing of the Tethys Seaway (Straume et al., 2020). Episodes of enhanced circulation of the AABW in the Atlantic during this timeframe are revealed by a hiatus corresponding to the Late Eocene (~40 Ma) (Wright and Miller, 1993) and by the accumulation of thick contourite drifts. These drifts have been found along the pathway of the modern AABW in the Eastern Atlantic, and among them are the drifts of Antarctica (Uenzelmann-Neben et al., 2022), Agulhas Ridge (Schut et al., 2002; Schüt and Uenzelmann-Neben, 2005; Gruetzner and Uenzelmann-Neben, 2016), Ivory Coast Rise (Jones and Okada, 2006), Gabon (Séranne and Abeigne, 1999) and Guinea (Santhein and Faugères, 1993). In the Western Atlantic, the thick Newfoundland contourite drift began to develop under paleo-water depths of 4000-4500 m near the early-middle Eocene boundary (Boyle et al., 2017), while the Greater Antilles Outer Ridge started in the middle-late Eocene (Tucholke, 2002). The Outer Ridge drift began to accumulate near the EOT (Faugères and Stow, 2008). The onset of the Argentine (Hernández-Molina et al., 2009) and Uruguay drifts (Preu et al., 2012; 2013) is of similar age.

In the following phase, discontinuity D4 was overlain by sediments of seismic unit U4, which represent the continuation of contourite accumulation (Fig. 10, 11c). During this maintenance phase

the deposits kept the same lenticular shape as the precedent ones. Regional episodes of strengthening of the AABW during this time interval have been inferred from several hiatus in the Southern Atlantic, corresponding to earliest Oligocene (~36 Ma), middle Oligocene (~30 Ma), latest Oligocene (~24 Ma) and middle Miocene (~15 Ma) (Wright and Miller, 1993).

6.4.5 Stage III – CDS-2: Onset, growth and maintenance (Middle Miocene to Quaternary)

Discontinuity D5 testifies the main sedimentary change with the beginning of a new depositional stage (Fig. 10, 11d), demonstrating depocenter migration (Drift 1) toward shallower depths (Drift 2) (Fig. 11d). Usually, drift migration occurs either by lateral shifting of the current driven by oceanographic changes or due to local topographic obstacles (Hernández-Molina et al., 2008; 2009). The drift's migration reflects a profound change in the deep-water circulation in the study area near the middle Miocene, possibly due to both global and regional causes. The Middle Miocene is also the time of final closure of the Tethys Seaway (Bahr et al., 2022) and opening of deep-water connections between the Artic and North Atlantic and full initiation of a deep NADW (Hernández-Molina et al., 2022). The decreasing activity of the bottom current in the western sector is testified by the onlap of internal reflections of U5 against D5, burying Drift 1.. Regionally, the drift migration could have also been promoted by the build-up and uplift of the Madeira volcanic plateau, and local strengthening of bottom current benefiting the deposition of Drift 2 in since the Miocene.

Discontinuity D6 marks the onset of the last and youngest phase of contourite drift development offshore Madeira Island spanning from Late Pliocene to Quaternary. We suggest that it was formed by an erosional event in the Late Pliocene linked to enhancement of the AABW circulation (Fig. 10, 11d). In fact, intensification of the AABW circulation occurred after the onset of the Northern Hemisphere Glaciation at 2.74 Ma (e.g., Shackleton and Kennett, 1975; Raymo et al., 1996; Sykes et al., 1998; Kleiven et al., 2002; Bartoli, 2005; Mudelsee and Raymo, 2005) (. The alternating glacial-interglacial cycles that dominated the Quaternary imposed severe changes in the deep-water circulation, involving the AABW and NADW (e.g. Böhm et al., 2015; Matsumoto, 2017). It was under such climatic and paleoceanographic conditions that elapsed the growth stage of Drift 2

represented by the thick accumulation of seismic unit U6. The drift crest is located at ~3000-3900 m water depth, coinciding with present-day depth range of NADW circulation (~2000-4000 m water depth) rather than the AABW (> 4000 m water depth). But the NADW is a water mass lowing southward and therefore incompatible with the Drift 2 formation. An explanation for this paradox would be that Drift 2 is a relict feature deposited under oceanographic conditions distinct from the present-day ones. Moreover, its relict condition was proposed earlier by Embley et al. (1978). These authors based their deduction on the dominance of pelagic deposition in the late Pleistocene and on the scarce presence of bedforms typically shaped by bottom-currents, such as sediment waves, channels, scours, erosional grooves and furrows (e.g., Habgood et al., 2003; Ercilla et al., 2017). In fact, several studies indicate that during glacial periods there was an expansion of invigorated AABW and a reduction, or even suppression, of the NADW formation (e.g., Emery and Uchupi, 1984; Raymo et al., 1996; Ravelo and Andreasen, 2000; Lund et al., 2011; Böhm et al., 2015; Matsumoto, 2017). Thus, stronger NADW flowed during interglacial conditions, with a major peak recognized at ~2.0-1.5 Ma (Bell et al., 2015). By contrast, glacial periods were marked by production and spreading of invigorated, faster, saltier and voluminous AABW (Boyle and Keigwin, 1987; Duplessy et al., 1988; Lund et al., 2011). Moreover, several authors proposed that the AABW-NADW boundary, presently at ~4000 m water depth, shoaled to ~2000 m water depth during the Last Glacial Maximum (Lund et al., 2011; Adkins, 2013; Böhm et al., 2015; Matsumoto, 2017). There is evidence of a shallower AABW circulating in the West Portuguese margin during glacial stages as MIS 12 (Rodríguez-Tovar et al., 2015) while presently is bathed by the NADW. Bearing this in mind, we propose that deposition of unit U6 (<4000 m water depth) has been active during Quaternary glacial stages, when the AABW reached its maximal volume and vertical expansion (Fig. 12). During interglacial stages Drift 2 becomes inactive, as it is bathed only by the NADW and pelagic sedimentation dominates. This hypothesis agrees with other large drifts found in the South Atlantic and associated with the influence of a shallower and more vigorous AABW during glacial stages (e.g., Preu et al., 2012; 2013; Hernández-Molina et al., 2016). Therefore, offshore Madeira Island the enhancement of the AABW during the Quaternary climate cooling

periods favored contourite drift deposition preferentially on areas located around 3000 m water depth. Below 4000 m water depth, deposition was restricted to a field of small patch drifts associated with seafloor reliefs (Roque et al., 2022).

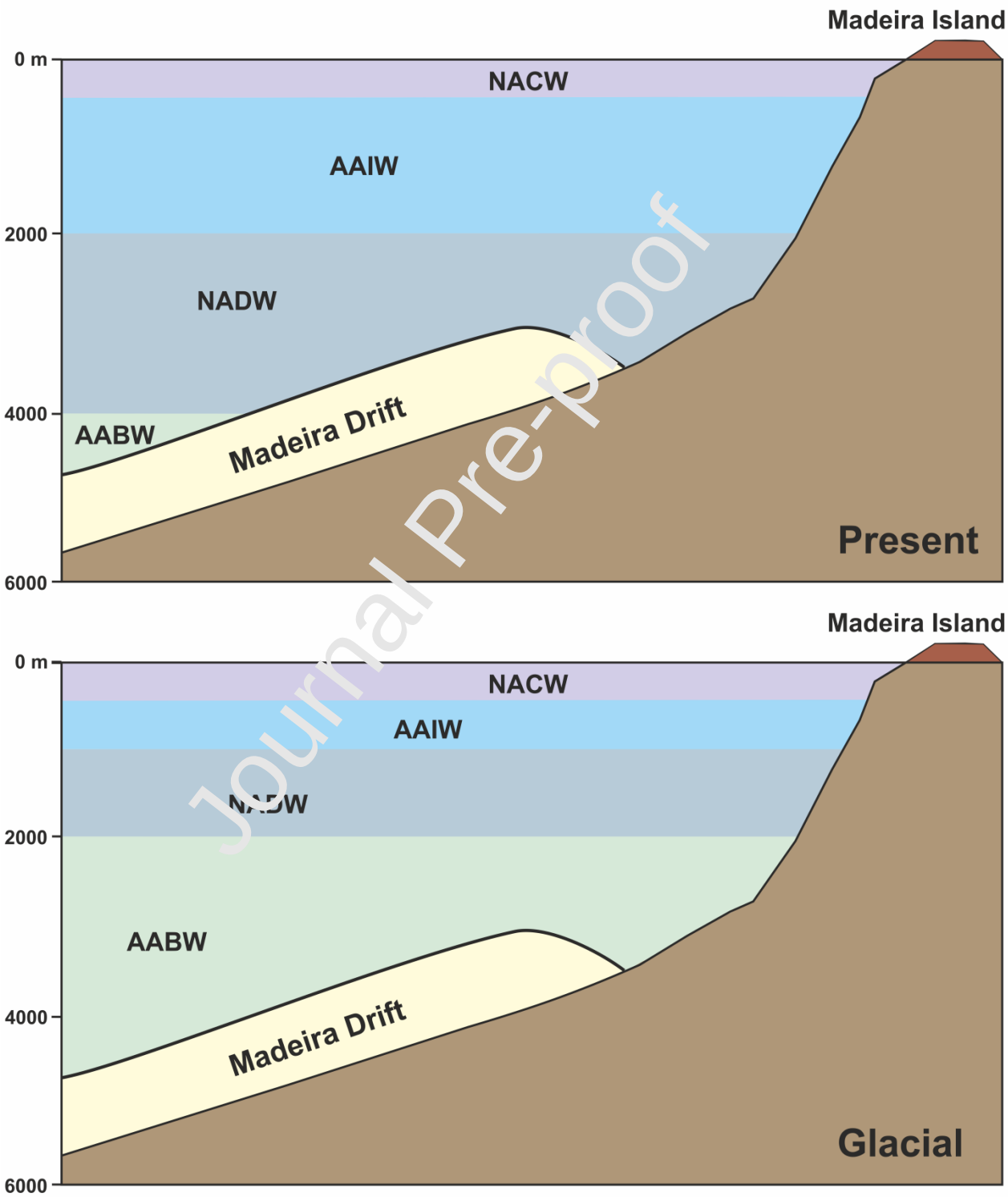

Figure 12 – Sketch showing the depth level of water masses circulation during the present (interglacial) and in glacial periods around Madeira Island slope where the Madeira CDSs are. Presently, Drift 2 is bathed by the NADW although its configuration indicates deposition under northward circulating water mass. According to several authors, the AABW was enhanced and expanded during glacials. We suggest that Drift 2 was deposited mainly during glacial periods by the circulation of the glacial AABW. Position of AABW and AAIW during glacials is based on Böhm et al. (2015) and Oppo and Curry (2012), respectively. See text for details.

After the deposition of U6, the Drift 2 has been affected by slope failure that disrupted this unit. This led to the formation of MTDoutcropping as seismic sub-unit U6a (Fig. 10, 11d). Itspreservation on the seafloorsuggests that slope-failure might have been active until recent times. This may indicate either that mass movements have been dominant during the Late Pliocene-Quaternary or, the circulation of a weak bottom-current prevented contourite deposition. Despite the well-known predisposition of contourite deposits for sliding (e.g., Bryn et al., 2005), it is impossible to determine the triggering mechanism for these debris flows. But, considering the geological and oceanographic settings of Madeira Island, two potential triggers can be discussed: i) the preconditioning imposed by the west-dipping basement and the tectono-magmatic activity; ii) the erosion provoked by the NADW when impinging the western flank of Drift 2 during interglacials. We suggest that the topography of the underlying oceanic basement has been a preconditioning factor for the occurrence of mass movements in the Drift 2 western flank. There, the basement consists of a large uplifted and tilted oceanic crust block that forms an extensive west-dipping surface, which could have favored landsliding. The tectono-magmatic activity in the Madeira Island might have also played an important role in triggering the debris flows. During the Late Pliocene and Quaternary the Madeira Island suffered ~500 m of uplift and several subaerial volcanism episodes with a peak at ~3.0 Myr ago followed by minor eruptions at 740, 620, 550 and 6.5 ka (Ribeiro and Ramalho, 2007; Ramalho et al., 2015). Under such conditions, the youngest sediments of Drift 2 (U6 and upper part of U5) could have failed as consequence of some of these tectono-magmatic episodes. Other potential trigger was the circulation of the NADW. Present-day deep-water circulation at these depths is dominated by the NADW, which intensified since ~0.9 Ma (Raymo et al., 1996) and possibly had a bigger erosional role, scouring the western flank of Drift 2. This might

have caused some instability making the Drift 2 prone to landsliding. Buried debris flows have also been recognized within sediments of Drift 2 located below 4000 m water depth (Roque et al., 2022).

7. Conclusions

The seismic stratigraphy analysis of multichannel seismic reflections profiles offshore Madeira Island in the NE-Central Atlantic allowed us to present the following conclusions.

1- New contourite depositional systems (CDS-1 and CDS-2) formed from Late Cretaceous (Campanian?) to Quaternary have been discovered in the NE-Central Atlantic offshore Madeira Island between ~3000 and ~4800 mwd. The CDS-1 represents the first evidence of earliest SCW incursions' in this region of the NE-Central Atlantic in the Late Cretaceous, while the CDS-2 reveals the fluctuations of the AABW circulation during glacials and interglacials.

2- The deposition of these CDSs reflects the role played by different scale factors in the bottom current dynamics though time. At global scale, the development of both CDSs has been dependent of plate tectonics dynamics, which leaded to the opening or closure of ocean gateways and consequent paleoclimatic and paleoceanographic changes. At regional scale, they seem to be linked to the tectono-magmatic activity of Madeira mantle plume, which culminated in the Late Miocene with uplift and formation of the Madeira Island. Locally, the resulting submarine volcanic edifice acted as an obstacle to the northward flowing SCW and AABW and favored the accumulation of both CDSs through time.

3- The CDS-1 and CDS-2 provide a good record of erosional surfaces linked to changes in deepwater masses strength's through time. They represent a promising site to better understand the evolution of deep-water circulation since the Late Cretaceous, helping to fill gaps in the knowledge of this sector of the Central Atlantic.

Acknowledgements

We acknowledge the FCT financial support through project UIDB/50019/2020 – IDL (Associated Laboratory).This study was conducted in the framework of "The Drifters Research Group" of the Department of Earth Sciences, Royal Holloway University of London (UK).

Data Availability Statement

The data that support this study has been provided by EMEPC (Task Group for the Extension of Continental Shelf, Portugal). Restrictions concerning to the availability of these data may be applied since they are included in the Portuguese Submmisson to the CLCS, UN and currently under evaluation. We also thank the Editor and Gabriel Tagliaro and Daniele Casalbore for their helpful reviews, which improved greatly the quality of our manuscript.

References

Abranches, M.C., Storetvedt, K.M.1984. Paleomagnetic evidence for the origin of Madeira. Physics of the Earth and Planetary Interiors, 34, 137-149. http://doi.org/10.1016/0031-9201(84)90002-5.

Adkins, J.F.2013. The role of deep ocean circulation in setting glacial climates. Paleoceanography, 28, 539–561. http://doi:10.1002/palo.20046.

Arhan, M., Colin de Verdière, A., Mémery, L. 1994. The eastern boundary of the subtropical North Atlantic. J. Phys. Oceanogr. 24, 1295-1316.

Bahr, A., Kaboth-Bahr, S., Karas, C., 2021. The opening and closure of oceanic seaways during the Cenozoic: pacemaker of global climate change?. Geo. Soc. London Spec. Publ. 523, http://doi.org/10.1144/SP523-2021-54.

Bartoli, G. Sarnthein, M., Weinelt, M., Erlenkeuser, H., Garbe-Schönberg, D., Lea, D.W. 2005. Final closure of Panama and the onset of northern hemisphere glaciation. Earth Planet. Sci. Lett. 237, 33– 44. http://doi:10.1016/j.epsl.2005.06.020

Barton, E.D. 2001. Canary and Portugal currents. In: Ocean currents: a derivative of the Encyclopedia of Ocean Sciences.(eds) J.H. Steele, S.A. Thorpe, K.K. Turekian. 44-53. http://doi:10.1006/rwos.2001.0360.

Bell, D.B., Simon J.A. Jung, Dick Kroon. 2015. The Plio-Pleistocene development of Atlantic deep-water circulation and its influence on climate trends. Quat. Sci. Rev. 123, 265-282.

Berggren, W.A., Aubry, M.-P., Van Fossen, M., Kent, D.V., Norris, R.D., and Quillévéré, F., 2000. Integrated Paleocene calcareous plankton magnetobiochronology and stable isotope stratigraphy: DSDP Site 384 (NW Atlantic Ocean). Palaeogeogr., Palaeoclimatol., Palaeoecol., 159, 1–51. http://doi:10.1016/S0031-0182(00)00031-6.

Billups, K. 2002 Late Miocene through early Pliocene deep water circulation and climate change viewed from the sub-Antarctic South Atlantic. Palaeogeogr., Palaeoclimatol., Palaeoecol., 185, 287-307.

Bird, D.E., Hall, S.A., Burke, K., Casey, J.F., Sawyer, D.S. 2007 Early Central Atlantic Ocean seafloor spreading history. Geosphere, 3, 5, 282–298. http://doi: 10.1130/GES00047.1.

Böhm, E., Lippold, J., Gutjahr, M., Frank, M., Blaser, P., Antz, B., Fohlmeister, J., Frank, N., Andersen, M.B., Deininger, M. 2015. Nature 517, 73-76. http://doi:10.1038/nature14059.

Borrelli, C., Cramer, B.S., Katz, M.E. 2014. Bipolar Atlantic deepwater circulation in the middle-late Eocene: Effects of Southern Ocean gateway openings, Paleoceanography, 29, 308–327, http://doi:10.1002/2012PA002444.

Boyle, E.A., Keigwin, L.1987. North Atlantic thermohaline circulation during the past 20,000 years linked to high-latitude surface temperatures. Nature, 330, 35-40.

Boyle P.R., Romans, B.W., Tucholke, B.E. Norris, R.D., Swift, S.A., Sexton, P.F. 2017. Cenozoic North Atlantic deep circulation history recorded in contourite drifts, offshore Newfoundland, Canada. Mar. Geol. 385, 185–203.

Bryn, P., Berg, K., Stoker, M.S., Haflidason, H., Solheim, A. 2005. Contourites and their relevance for mass wasting along the Mid-Norwegian Margin. Mar. Petrol. Geol. 22, 85–96.

Camerlengui, A., Rebesco, M. (2008). Contourites. Developments in Sedimentology, Volume 60. ISSN 0070-4571. http://doi: 10.1016/S0070-4571(08)00201-X.

Campbell, D.C., Mosher, D.C. 2016. Geophysical evidence for widespread Cenozoic bottom current activity from the continental margin of Nova Scotia, Canada. Mar. Geol. 378, 237–260. http://dx.doi.org/10.1016/j.margeo.2015.10.005.

Comas-Rodríguez, I., A. Hernández-Guerra, E. Fraile-Nuez, A. Martínez-Marrero, V. M. Benítez-Barrios, M. D. Pérez-Hernández, and P. Vélez-Belchí (2011), The Azores Current System from a meridional section at 24.5°W. J. Geophys. Res., 116, C09021, doi:10.1029/2011JC007129.

Cornen, G., Girardeau, J., Agrinier, P., Grasset, O., Hinschberger, F., Loyen, H., Malod, J., Matias, L., Monteiro, J., Pinheiro, L.. de Quillacq, B., Ribeiro, A., Thinon, I. 2003. Campagne Tore–Madère: Premiers résultats. 110 p.

Crosby, A.G., McKenzie, D., Sclater, J.G. 2006. The relationship between depth, age and gravity in the oceans. Geophys. J. Int. 166, 553–573. doi: 10.1111/j.1365-246X.2006.03015.x.

Diekmann, B., Kuhn, G., Gersonde, R., Mackensen, A. 2004. Middle Eocene to early Miocene environmental changes in the sub-Antarctic Southern Ocean: evidence from biogenic and terrigenous depositional patterns at ODP Site 1090. Glob. Planet. Chang. 40, 295–313, doi:10.1016/j.gloplacha.2003.09.001.

Donnadieu, Y., Pucéat, E., Moiroud, M., Guillocheau, F., Deconinck. J-F. 2016. A better-ventilated ocean triggered by Late Cretaceous changes in continental configuration. Nat. Comm., 7:10316 DOI: 10.1038/ncomms10316.

Dunlap, D.B., Wood, L.J., Moscardelli, L.G. 2013. Seismic geomorphology of early North Atlantic sediment waves, offshore northwest Africa. Interpretation, 1, SA75–SA91. http://dx.doi.org/10.1190/INT-2013-0040.1.

Duplessy, J.C., Shackleton, N.J., Fairbanks, R.G., Labeyrie, L., Oppo, D., Kallel, N. 1988. deepwater source variations during the last climatic cycle and their imp act on the global deepwater circulation. Paleoceanography, 3, 343-360.

Dutkiewicz, A., Müller, R. D. 2022. The history of Cenozoic carbonate flux in the Atlantic Ocean constrained by multiple regional carbonate compensation depth reconstructions. Geochemistry, Geophysics, Geosystems, 23, e2022GC010667. https://doi.org/10.1029/2022GC010667

Embley, R.W., Rabinowitz , P.D., Jacobi, R.D.1978.Hyperbolic echo zones in the eastern Atlantic and the structures of the southern Madeira Rise. Earth Planet. Sci. Lett. 41, 418-433

Emery, K.O., Uchupi, E. 1984. The geology of the Atlantic Ocean. 855-856 Spriger-Verlag.

Ercilla, G., Casas, D., Hernández-Molina, F.J., Roque, C. 2017. Generation of bedforms by the Mediterranean Outflow current at the exit of the Strait of Gibraltar. In: Guillén, J., Acosta, J., Chiocci, F.L., Palanques, A. Springer Internation Publishing Switzeland, pp. 273-280. DOI 10.1007/978-3-319-33940-5_42.

Faugères, J-C., Stow, D.A.V., Imbert, P., Viana, A. 1999. Seismic features diagnostic of contourite drifts. Mar. Geol. 162, 1–38.

Faugères, J.C., Stow, D.A.V., 2008. Contourite drifts: nature, evolution and controls. In: Rebesco, M., Camerlenghi, A. (Eds.), Contourites Developments in Sedimentology vol. 60. Elsevier, pp. 259–288.

Ferreira, D., Cessi, P., Coxall, H.K., de Boer, A., Dijkstra, H.A., Drijfhout, S.S., Eldevik, T., Harnik, N., McManus, J.F., Marshall, D.P., Nilsson, J., Roquet, F., Schneider, T., Wills, R.C. 2018. Atlantic-Pacific Asymmetry in Deep Water Formation. Annu. Rev. Earth Planet. Sci. 46:327–52. https://doi.org/10.1146/annurev-earth-082517-010045.

Fleischmann, U., Hildebrandt, H., Petrika, A., Bayer, R. 2001. Transport of newly ventilated deep water from Iceland Basin in the Westeuropean Basin, Deep-sea Res. part I, 48, 1793-1819. Doi:10.1016/S0967-0637(00)00107-2.

Flower, B.P. J.C., Zachos, Pau, H. 1997. Milankovitch-scale climate variability recorded near the Oligocene-Miocene boundary. IN Shackleton, N.J., Curry, W.B., Richter, C., Bralower, T.J., (Eds.) 1997. Proc. ODP. Sci. Results, 154: College Station, TX (Ocean Drilling Program), pp.433-440. Doi:10.2973/odp.proc.sr.154.141.1997.

Föllmi, K.B. 2012. Early Cretaceous life, climate and anoxia. Cretac. Res. 35. 230-257. doi:10.1016/j.cretres.2011.12.005.

Friedrich, O., Erbacher, J., Moriya, K., Wilson, P.A., Kuhnert, H. 2008. Warm saline intermediate waters in the Cretaceous tropical Atlantic Ocean. Nature Geosci. 1. 453-457.

Friedrich, O., Norris R.D., Erbacher, J. 2012. Evolution of middle to Late Cretaceous oceans-A 55 m.y. record of Earth's temperature and carbon cycle. Geology, 40, 107-110. doi: 10.1130/G32701.1.

Fründt, B., Waniek, J.J., 2012. Impact of the Azores Front propagation on deep Ocean particle flux. Cent. Eur. J. Geosci. 4, 531-544.

Geldmacher, J., Hoernle, K. 2000. The 72 Ma Geochemical Evolution of the Madeira hotspot (eastern North Atlantic): recycling of Palaeozoic (≤500 Ma) basaltic and gabbroic crust, Earth Planet. Sci. Lett. 183, 73– 92.

Geldmacher, J., Hoernle, K., Bogaard, P.v.d, Zankl, G., Garbe-Schönberg, D. 2001. Earlier history of the ≥70 Ma old Canary hotspot based on the temporal and geochemical evolution of the Selvagen archipelago and neighboring seamounts in the eastern North Atlantic, J. Volcanol. Geotherm. Res. 111, 55– 87.

Geldmacher, J., Hoernle, K., Bogaard, P.v.d., S. Duggen, R. Werner. 2005. New 40Ar/ 39Ar age and geochemical data from seamounts in the Canary and Madeira volcanic provinces: Support for the mantle plume hypothesis. Earth Planet. Sci. Lett. 23, 85– 101. doi:10.1016/j.epsl.2005.04.037.

Glazkova, T., Hernández-Molina, F.J., et al., 2022. Sedimentary processes in the Discovery Gap (Central-NE Atlantic): An example of a deep marine gateway. Deep-Sea Res. 180, 103681.

Goldner, A., Herold, N., Huber, M. 2014. Antarctic glaciation caused ocean circulation change at the Eocean-Oligocene transition. Nature, 511, 574-578.

Granot, R., Dyment, J. 2015. The Cretaceous opening of the South Atlantic Ocean. Earth Planet. Sci. Lett. 414, 156–163. http://dx.doi.org/10.1016/j.epsl.2015.01.015.

Gruetzner, J., Uenzelmann-Neben, G. 2016 Contourite drifts as indicators of Cenozoic bottom water intensity in the eastern Agulhas Ridge area, South Atlantic. Mar. Geol. 378, 350-360.

Habgood, E.L., Kenyon, N.H., Masson, D.G., Akhmetzhanov, A., Weaver, P.P.E., Gardner, J., Mulder, T. 2003. Deep-water sediment wave fields, bottom current sand channels and gravity flow channel-lobe systems: Gulf of Cadiz, NE Atlantic. Sedimentology, 50, 483–510.

Hall, I. R., McCave, I.N., Zahn, R., Carter, L., Knutz, P.C., Weedon, G.P. 2003. Paleocurrent reconstruction of the deep Pacific inflow during the middle Miocene: Reflections of East Antarctic Ice Sheet growth, Paleoceanography, 18(2), 1040, doi:10.1029/2002PA000817.

Hassold, N.J.C., Rea, D.K., van der Pluijm, B.A., Parés, J.M. 2009. A physical record of the Antarctic Circumpolar Current: Late Miocene to recent slowing of abyssal circulation. Palaeogeogr. Palaeoclimatol, Palaeoecol 275, 28–36. doi:10.1016/j.palaeo.2009.01.011.

Haug, G.H., Tiedemann, R., 1998. Effect of the formation of the Isthmus of Panama on Atlantic Ocean thermohaline circulation. Nature 393, 673-676.

Hay, W.W. 2008. Evolving ideas about the Cretaceous climate and ocean circulation. Cretac. Res. 29, 725–753.

Hay, W., 2009. Cretaceous Oceans and Ocean Modeling. In: Hu, X., Wang, C., Scott, R.W., Wagreich, M., Jansa, L. (Eds.), Cretaceous Oceanic Red Beds: Stratigraphy, Composition, Origins, and Paleoceanographic and Paleoclimatic Significance. SEPM Spec. Publ. 91, pp. 243–271. https://doi.org/10.2110/sepmsp.091.

Hayes, D.E., Pimm, A.C. and Shipboard Scientific Party. 1972 Initial Report of Deep Sea Drilling Project, Leg 14, Washington, D.C., U.S. Government Printing Office.

Heezen, B.C., Tharp, M., Ewing, M. 1959. The floor of the oceans. The North Atlantic. Geol. Soc. Am., Special paper 65.

Heezen, B.C., Hollister, C.D., 1964. Deep sea current evidence from abyssal sediments. Mar. Geol. 1, 141–174.

Hollister and Heezen 1972: Hollister, C.D., Heezen, B.C., 1972. Geological effects of ocean bottom currents: western North Atlantic. In: Gordon, A.L. (Ed).., Studies in Physical Oceanography, Vol. 2. Gordon and Breach, New York, 37–66.

Hernández-Molina, F.J., Maldonado, A., Stow, D.A.V., 2008. Abyssal plain contourites, In: M. Rebesco, A. Camerlenghi (Eds.), Contourites. Developments in Sedimentology 60, Elsevier, pp. 345-378. https://doi.org/10.1016/S0070-4571(08)10018-8.

Hernández-Molina, F.J., Paterlini, M., Violante, R., Marshall, P., de Isasi, M., Somoza, L., Rebesco, M. 2009. Contourite depositional system on the Argentine Slope: An exceptional record of the influence of Antarctic water masses. Geology, 37, p. 507–510; doi:10.1130/G25578A.1.

Hernández-Molina, F.J., Paterlini, M., Somoza, L., Violante, R., Arecco, M.A., de Isasi, M. , Rebesco, M., Uenzelmann-Neben, G., Neben, S., Marshall, P.2010. Giant mounded drifts in the Argentine Continental Margin: Origins, and global implications for the history of thermohaline circulation. Mar. Petrol. Geol. 27, 1508-1530. doi:10.1016/j.marpetgeo.2010.04.003.

Hernández-Molina, F.J., Serra, N., Stow, D.A.V., Llave, E., Ercilla, G., Van Rooij, D. 2011. Along-slope oceanographic processes and sedimentary products around the Iberian margin. Geo-Mar Lett, 31, 315–34.1DOI 10.1007/s00367-011-0242-2.

Hernández-Molina, F.J., de Castro, S., de Weger, W., Duarte, D., Fonnesu, M, Glazkova, T., Kirby, A., Llave, E., Ng, Z.L., Mantilla Muñoz, O., Rodrigues, S., Rodríguez-Tovar, F.J., Thieblemont, A., Viana, A., Yin, S. , 2022. Chapter 9: Contourites and mixed depositional systems: a paradigm for deepwater sedimentary environments. In: Deep-Water Depositional Systems. (Eds.: Rotzien, J.R., Yeilding, C., Sears, R., Catuneanu, O., Hernández-Molina, F.J.,). Elservier, 301-360. https://doi.org/10.1016/B978-0-323-91918-0.00004-9.

Hoernle, K., Zhang, J-S., Graham, D. 1995. Seismic and geochemical evidence for large-scale mantle upwelling beneath the eastern Atlantic and Western and Central Europe. Nature, 374, 34-39.

Hollister, C.D., Heezen, B.C., 1972. Geological effects of ocean bottom currents: Western North Atlantic. In: Gordon, A.L. (Ed.), Studies in Physical Oceanography, 2. Gordon and Breach, New York, pp. 37–66.

Huang, X., M. Stärz, K. Gohl, G. Knorr, and G. Lohmann (2017), Impact of Weddell Sea shelf progradation on Antarctic bottom water formation during the Miocene, Paleoceanography, 32, 304–317, doi:10.1002/2016PA002987.

Huber, M., Nof, D. 2006. The ocean circulation in the southern hemisphere and its climatic impacts in the Eocene. Palaeogeogra, Palaeoclimatol, Palaeoecol. 231, 9-28.doi:10.1016/j.palaeo.2005.07.037.

Huber, M., Brinkhuis,H., Stickley, C.E., Döös, K., Sluijs, A., Warnaar, J., Schellenberg, S.A., Williams, G.L. 2004. Eocene circulation of the Southern Ocean: Was Antarctica kept warm by subtropical waters? Paleoceanography, 19, PA4026, doi:10.1029/2004PA001014.

Huber, B.T., MacLeod, K.G., Watkins, D.K., Coffin, M.F. 2018. The rise and fall of the Cretaceous Hot Greenhouse climate. Glob. Planet. Chang. 167, 1–23. https://doi.org/10.1016/j.gloplacha.2018.04.004.

Hüneke, H., Henrich, R., 2011. Chapter 4 - Pelagic Sedimentation in modern and Ancient Oceans. In: Heiko, H., Thierry, M. (Eds.), Deep-Sea Sediments, Developments in Sedimentology, 63. Elsevier, pp. 215–351.

Hunt, J.E., Wynn, R.B., Talling, P.J., Masson, D.G. 2013. Frequency and timing of landslide triggered turbidity currents within the Agadir Basin, offshore NW Africa: Are there associations with climate change, sea level change and slope sedimentation rates? Mar. Geol. 346, 274–291. http://dx.doi.org/10.1016/j.margeo.2013.09.004.

Hunter, S., Wilkinson, D., Louarn, E., McCave, I.N., Rohling, E., Stow, D.A.V., Bacon, S. 2007. Deep western boundary current dynamics and associated sedimentation on the Eirik Drift, Southern Greenland Margin. Deep-Sea Res154, 2036–2066. doi:10.1016/j.dsr.2007.09.007.

Hutchinson, D.K., Coxall, H.K., Lunt, D.J., Steinthorsdottir, M., de Boer, A.M., Baatsen, M., von der Heydt, A., Huber, M., Kennedy-Asser, A.T., Kunzmann, L., Ladant, J-B., Lear, C.H., Moraweck, K., Pearson, P.N., Piga, E., Pound, M.J., Salzmann, U., Scher, H.D., Sijp, W.P., Śliwińska, K.K., Wilson, P.A., Zhang, Z . 2020. The Eocene-Oligocene transition: a review of marine and terrestrial proxy data, models and model-data comparisons. Clim. Past. https://doi.org/10.5194/cp-2020-68

Jenkyns, H. C. 2010. Geochemistry of oceanic anoxic events, Geochem. Geophy. Geosy., 11, Q03004, https://doi.org/10.1029/2009gc002788.

Jones E.J.W, Okada, H. 2006. Abyssal circulation change in the equatorial Atlantic: Evidence from Cenozoic sedimentary drifts off West Africa. Mar. Geol. 232, 49–61. doi:10.1016/j.margeo.2006.07.002.

Jones, E. J. W., Bigg, G. R., Handoh, I. C., Spathopoulos, F., 2007. Distribution of deep-sea black shales of Cretaceous age in the eastern Equatorial Atlantic from seismic profiling, Palaeogeogr, Palaeoclimatol, Palaeoecol, 248, 233–246.

Kleiven, H.F., Jansen, E., Fronval, T., Smith, T.M. 2002. Intensification of Northern Hemisphere glaciations in the circum Atlantic region (3.5-2.4 Ma)-ice-rafted detritus evidence. Palaeogeogr, Palaeoclimatol, Palaeoecol, 184, 213-223.

Knutz, P.C. 2008. Palaeoceanographic significance of contourite drifts. Developments in Sedimentology, Volume 60, 511-535. ISSN 0070-4571, DOI: 10.1016/S0070-4571(08)00224-0.

Ladant, J-B., Poulsen, C.J., Fluteau, F., Tabor, C.R., MacLeod, K.G., Martin, E.E., Haynes, S.J., Rostami, M.A. 2020. Paleogeographic controls on the evolution of Late Cretaceous ocean circulation. Clim. Past, 16, 973–1006, 2020 https://doi.org/10.5194/cp-16-973-2020

Lagabrielle, Y., Goddéris, Y., Donnadieu, Y., Malavieille, J., Suarez, M. 2009.The tectonic history of Drake Passage and its possible impacts on global climate, Earth Planet. Sci. Lett., 279, 197– 211, https://doi.org/10.1016/j.epsl.2008.12.037, 2009.

Lancelot, Y., Seibold, E. and Shipboard Scientific Party. 1978. Initial Report of Deep Sea Drilling Project, Leg 41, Washington, D.C., U.S. Government Printing Office.doi:10.2973/dsdp.proc.41.1978.

Lancelot, Y., Seibold, E.1978.The evolution of the Central Northeastern Atlantic-summary of results of DSDP Leg 41. 1215-1245. Doi:10.2973/dsdp.proc.41.151.1978.

Lawver, A.L., Gahagan, L.M., 2003. Evolution of Cenozoic seaways in the circum-Antarctic region. Palaeogeogr, Palaeoclimatol, Palaeoecol, 198, 11-37. doi:10.1016/S0031-0182(03)00392-4.

Livermore, R., Hillenbrand, C.-D., Meredith, M. Eagles, G. 2007. Drake Passage and Cenozoic climate: An open and shut case? Geochemistry, Geophys. Geosystems, 8, Q01005, doi:10.1029/2005GC001224.

Louarn, E. and Morin, P.: Antarctic Intermediate Water Influence on Mediterranean Sea Water Outflow, Deep-Sea Res. I, 58, 932–942, https://doi.org/10.1016/j.dsr.2011.05.009, 2011.

Lund, D.C., Adkins, J.F., Ferrari, R. 2011. Abyssal Atlantic circulation during the Last Glacial Maximum: Constraining the ratio between transport and vertical mixing. Paleoceanography, 26, PA1213, doi:10.1029/2010PA001938.

Luo, Y., Tjiputra, J., Guo, C., Zhang, Z., Lippold., J. 2018. Atlantic deep water circulation during the last interglacial. Nature Scientific Reports 8-4401. doi:10.1038/s41598-018-22534-z.

MacLeod, K. G., Isaza Londoño, C., Martin, E.E., Jiménez Berrocoso, Á., Basak, C. 2011. Changes in North Atlantic circulation at the end of the Cretaceous greenhouse interval, Nat. Geosci., 4, 779–782, doi:10.1038/ngeo1284.

MaKay, R., Naish, T., Carter, L., Riesselman, C., Dunbar, R., Sjunneskog, C., Winter, D., Sangiorgi, F., Warren, C., Pagani, M., Schouten, S., Willmott, V., Levy, R., DeConto, R., Powell. R.D. 2012. Antarctic and Southern Ocean influences on Late Pliocene global cooling. PNAS 109(17), 6423-6428. doi:10.1073/pnas.1112248109.

Martin, E.E., MacLeod, K.G., Jiménez Berrocoso, A., Bourbon, E. 2012. Water mass circulation on Demerara Rise during the Late Cretaceous based on Nd isotopes. Earth Planet. Sci. Lett. 327-328 (2012) 111–120. doi:10.1016/j.epsl.2012.01.037.

Mata, J., Fonseca, P., Prada, S., Rodrigues, D., Martins, S., Ramalho, R., Madeira, J., Cachão, M., Marques da Silva, C., Matias, M.J. 2013. O arquipélago da Madeira, in: Dias, R., Araújo, A., Terrinha, P., Kullberg, J.C. (Eds.), Geologia de Portugal, Volume II – Geologia Meso-cenozóica de Portugal. Escolar Editora, pp. 691-746.

Matos, C., Silveira, G., Matias, L., Caldeira, R., Ribeiro, M.L., Dias, N.A., Krüger, F., Bento dos Santos, T., 2015. Upper crustal structure of Madeira Island revealed from ambient noise tomography. J. Volcanol. Geotherm Res. 298, 136–145.

Matsumoto, K. 2017. Tantalizing evidence for the glacial North Atlantic bottom water. PNAS 114, 2794 2796. doi/10.1073/pnas.1701563114.

Merle, R., Schärer, U., Girardeau, J., Cornen, G. 2006. Cretaceous seamounts along the continent–ocean transition of the Iberian margin: U–Pb ages and Pb–Sr–Hf isotopes. Geochimica et Cosmochimica Acta 70, 4950–4976. doi:10.1016/j.gca.2006.07.004.

Miller, K.G., Kominz, M.A., Browning, J.V., Wright, J.D., Mountain, G.S., Katz, M.E., Sugarman, P.J., Cramer, B.S., Christie-Blick, N., Pekar, S.F., 2005. The Phanerozoic record of global sea-level change. Science 310, 1293–1298.

Miller, K.G., Wright, J.D., Katz, M.E., Wade, B.S., Browning, J.V., Cramer, B.S., and Rosenthal, Y., 2009, Climate threshold at the Eocene-Oligocene transition: Antarctic ice sheet influence on ocean circulation, *in* Koeberl, C., and Montanari, A., eds., The Late Eocene Earth-Hothouse, Icehouse, and Impacts: Geol. Soc. Am. Special Paper 452, p. 169–178, doi: 10.1130/2009.2452(11).

Moebius, I., Friedrich, O., Scher, H.D. 2014. Changes in Southern Ocean bottom water environments associated with the Middle Eocene Climatic Optimum (MECO). Palaeogeogr, Palaeoclimatol, Palaeoecol, 405, 16–27.

Moiroud, M., Pucéat, E., Donnadieu, Y., Bayon, G., Guiraud, M., Voigt, S., Deconinck, J-F., Monna, F. 2016. Evolution of neodymium isotopic signature of seawater during the Late Cretaceous: Implications for intermediate and deep circulation. Gondwana Research 36, 503–522. http://dx.doi.org/10.1016/j.gr.2015.08.005.

Mountain, G.S., Miller, K.G. 1992. Seismic and geological evidence for early Paleogene deepwater circulation in the western North Atlantic. Paleoceanography, 7, 423-439.

Mourlot, Y., Calvès, G., Clift, P.D., Baby, G., Chaboureau, A-C., Raisson, F. 2018. Seismic stratigraphy of Cretaceous eastern Central Atlantic Ocean: Basin evolution and palaeoceanographic implications. Earth Planet. Sci. Lett. 499, 107–121.

Mudelsee, M., Raymo, M.E. 2005. Slow dynamics of the Northern Hemisphere glaciation. Paleoceanography, 20, PA4022, doi:10.1029/2005PA001153.

Müller, R. D., Sdrolias, M., Gaina, C. , Roest, W. R. 2008. Age, spreading rates, and spreading asymmetry of the world's ocean crust, Geochem. Geophys. Geosyst., 9, Q04006, doi:10.1029/2007GC001743.

Murphy, D. P., and D. J. Thomas (2013), The evolution of Late Cretaceous deep-ocean circulation in the Atlantic basins: Neodymium isotope evidence from South Atlantic drill sites for tectonic controls, Geochem. Geophys. Geosyst., 14, 5323–5340, doi:10.1002/2013GC004889.

Nielsen, T., Knutz, P.C., Kuijpers, A., 2008. Seismic expression of contourite depositional systems. In: Rebesco, M., Camerlenghi, A. (Eds.), Contourites. Developments in Sedimentology 60. Elsevier, pp. 301–321.

Niemi, T.M., Ben-Avraham, Z., Hartnady, C.J.H., Reznikov, M. 2000. Post-Eocene seismic stratigraphy of the deep ocean basin adjacent to the southeast African continental margin: a record of geostrophic bottom current systems. Mar. Geol. 162, 237–258.

Nisancioglu, K.H., Raymo, M.E., Stone, P.H. 2003. Reorganization of Miocene deep water circulation in response to the shoaling of the Central American Seaway. Paleoceanography, 18, 1006, doi:10.1029/2002PA000767.

Norris, R.D., Wilson, P.A., Blum, P. 2011. Paleogene Newfoundland sediment drifts. IODP Sci. Prosp., 342. doi:10.2204/iodp.sp.342.2011.

Oppo, D.W., Curry, W.B. 2012. Deep Atlantic circulation during the Last Glacial Maximum and deglaciation. Nature Education Knowledge, 3 (10), 1.

Otto-Bliesher, B.L., Brady, E.c., Shields, C. 2002. Late Cretaceous ocean: coupled simulations with the National Center for Atmospheric Research Climate System model. Journal of Geophysical Research 107, D2, 10.1029/2001JD000821.

Palcu DV, Muraszko JR, Jaqueto PF and Jovane L. 2020. The Birth of a Connected South Atlantic Ocean: A Magnetostratigraphic Perspective. Front. Earth Sci. 8:375. doi: 10.3389/feart.2020.00375.

Peliz, A., Dubert, J., Santos, A.M.P., Oliveira, P.B., Le Cann, B., 2005. Winter upper ocean circulation in the Western Iberian Basin – Fronts, Eddies and Poleward Flows: an overview. Deep Sea Res. Part I: Oceanographic Research Papers 52, 621-646.

Pérez-Díaz, L., Eagles, G. 2017. South Atlantic paleobathymetry since early Cretaceous. Nature Scientific Reports, 7: 11819, DOI:10.1038/s41598-017-11959-7.

Pak, D.K., Miller, K.G. 1992. Paleocene to Eocene benthic foraminiferal isotopes and assemblages: Implications for deepwater circulation, Paleoceanography 7, 405-422.

Pinet, P.R. 2011. Initiation to Oceanography. Jones and Bartlett Publishers. pp.600

Potter, P.E., Szatmari, P. 2009. Global Miocene tectonics and the modern world. Earth Sci. Rev. 96, 279–295. doi:10.1016/j.earscirev.2009.07.003.

Poulsen, C.J., Barron, E.J., Arthur, M.A., Peterson, W.H. 2001. Response of the mid-Cretaceous global oceanic circulation to tectonic and CO2 forcings. Paleoceanography,16, 576–592.

Preu, B., Schwenk, T., Hernández-Molina, F.J., Violante, R., Paterlini, M., Krastel, S., Tomasini, J., Spieß, V. 2012. Sedimentary growth pattern on the northern Argentine slope: The impact of North Atlantic Deep Water on southern hemisphere slope architecture. Mar. Geol. 329–331, 113–125. http://dx.doi.org/10.1016/j.margeo.2012.09.009.

Preu, B., Hernández-Molina, F.J., Violante, R., Piola, A.R., Paterlini, C.M., Schwenk, T., Voigt, I., Krastel, S., Spiess, V. 2013. Morphosedimentary and hydrographic features of the northern Argentine margin: The interplay between erosive, depositional and gravitational processes and its conceptual implications. Deep-Sea Res. 75, 157–174. http://dx.doi.org/10.1016/j.dsr.2012.12.013

Ravelo, A.C., Andreasen, D., 2000. Enhanced circulation during a warm period. Geophys. Res. Lett. 27, 1001-1004.

Ramalho, R.S., Winckler, G., Madeira, J., Helffrich, G.R., Hipólito, A., Quartau, R., Adena, K., Schaefer, J.M. 2015. Hazard potential of volcanic flank collapses raised by new megatsunami evidence. Sci. Adv. 1:e1500456.

Raymo, M.E., Grant, B., Horowitz, M., Rau, G.H. 1996. Mid-Pliocene warmth: stronger greenhouse and stronger conveyor. Marine Micropaleontol. 27, 313-326.

Rebesco, M., Hernández-Molina, F.J., Van Rooij, D., Wåhlin, A., 2014. Contourites and associated sediments controlled by deep-water circulation processes: state-of-the-art and future considerations. Mar. Geol. 352, 111–154.

Rebesco, M., Camerlenghi, A., 2008. Contourites. Dev. Sedimentol. 60. Elsevier, Amsterdam.

Ribeiro, M. L., Ramalho, M., 2009. Uma visita geologica ao arquipelago da Madeira. Principais locais Geo-Turisticos, INETInovacao, Laboratorio Nacional de Energia e Geologia, 91 pp.

Robinson, S. A., Murphy, D.P., Vance, D., Thomas, D.J. 2010. Formation of 'Southern Component Water' in the Late Cretaceous: Evidence from Nd-isotopes, Geology, 38. 871–874, doi:10.1130/G31165.1.

Robinson, S.A., Vance, D. 2012. Widespread and synchronous change in deep-ocean circulation in the North and South Atlantic during the Late Cretaceous. Paleoceanography, 27, PA1102, doi:10.1029/2011PA002240.

Rodrigues, S., Deptuck, M., Kendell, K, Campbell, C., Hernández-Molina, F.J., 2022. Cretaceous to Eocene mixed turbidite-contourite systems offshore Nova Scotia (Canada): spatial and temporal variability of down- and along-slope processes. Mar. Petrol. Geol. 138, 105572.https://doi.org/10.1016/j.marpetgeo.2022.105572.

Rodríguez-Tovar, F.J., Dorador, J.; Martin-Garcia, G.M., Sierro, F.J., Flores, J.A., Hodell, D.A. 2015. Response of macrobenthic and foraminifer communities to changes in deep-sea environmental conditions from Marine Isotope Stage (MIS) 12 to 11 at the "Shackleton Site". Glob. Planet. Chang. 133, 176–187.

Roemmich, D.H., Wunsch, C. 1985. Two transatlantic sections:Meridional circulation and heat flux in the sub-tropical North Atlantic Ocean. Deep Sea Res. 32, 619-644.

Roque C., Madureira, P., Hernández-Molina, F.J., Santos de Campos, A., Quartau, R., Carrara, G., Brandão, F., Vázquez, J.T., Somoza, L., 2015. Acoustic evidence of along-slope processes associated with mass movement deposits on the Madeira Island lower slope (Eastern Central Atlantic). VII Symposium MIA15, Malaga, Spain, 21-23 September 2015, p. 583-58.

Roque, C., Hernández-Molina, F.J., Madureira, P., Quartau, R., Magalhães, V., Brito, P., Vázquez, J.T., Somoza, L. 2022. Interplay of deep-marine sedimentary processes with seafloor morphology offshore Madeira Island (Central NE-Atlantic). Mar. Geol. 443, 106675.Roque, D., Parras-Berrocal, I., Bruno, M., Sanchez-Leal, R., Hernandez-Molina, F.J., 2019. Seasonal variability of intermediate water masses in the Gulf of Cadiz: Implications of the Antarctic and subarctic seesaw. Ocean Science, 15, 1381–1397. https://doi.org/10.5194/os-15-1381-2019.

Ruddiman, W., Sarnthein, M., Baldauf et al. 1988. Proc. ODP Initial Reports, 108, College Station, TX (Ocean Drilling Project). doi:10.2973.odp.proc.ir.108.1988.

Sabatino, N., Meyers, S.R., Voigt, S., Coccioni, R., Sprovieri, M. 2018. A new high-resolution carbon-isotope stratigraphy for the Campanian (Bottaccione section): Its implications for global correlation, ocean circulation, and astrochronology. Palaeogeogr., Palaeoclimatol, Palaeoecol. 489, 29–39. http://dx.doi.org/10.1016/j.palaeo.2017.08.026.

Sarnthein, M., Faugères, J.C., 1993. Radiolarian contourites record Eocene AABW circulation in the equatorial East Atlantic. Sediment. Geol. 82, 145–155.

Shackleton, N.J., Kennett, J.P., 1975. Late Cenozoic oxygen and carbon isotope changes at DSDP site 284: Implications for glacial history of the northern hemisphere and Antarctica. Init. Rep. Deep Sea Drill Proj. 29, 801-807.

Schmincke, H-U., 1982. Volcanic and chemical evolution of the Canary Island. IN: Seibold, e. (Ed.9 Geology of the northwest African margin. Springer, New York, pp.273-306.

Schmincke, H-U., Weaver, P.P.E., Firth, J.V. 1995. Proc. ODP Initial Reports, 157, College Station, TX (Ocean Drilling Project). Doi:10.2973/odp.proc.ir.157.1995.

Schut, E.W., Uenzelmann-Neben, G., Gersonde, R. 2002. Seismic evidence for bottom current activity at the Agulhas Ridge. Glob. Planet. Chang. 34, 185–198.

Schut, E.W., Uenzelmann-Neben, G. 2005. Cenozoic bottom current sedimentation in the Cape basin, South Atlantic. Geophys. J. Int. 161, 325–333. doi: 10.1111/j.1365-246X.2005.02578.x.

Schwarz, S., Klügel, A., van den Bogaard, P., Geldmacher , J. 2005. Internal structure and evolution of a volcanic rift system in the eastern North Atlantic: the Desertas rift zone, Madeira archipelago. J. Volcanol. Geotherm. Res. 141, 123–155. doi:10.1016/j.jvolgeores.2004.10.002.

Searle, R.C., Schultheiss, P.J., Weaver, Noel, M., Kidd, R.B., Jacobs, C.L., Huggett, Q.J., 1985. Great Meteor East (distal Madeira Abyssal Plain): geological studies of its suitability for disposal of heat-emitting radioactive waste. IOS, Report 193, 162 pp. Séranne, M., Abeigne, C.R.N. 1999. Oligocene to Holocene sediment drifts and bottom currents on the slope of Gabon continental margin (west Africa) Consequences for sedimentation and southeast Atlantic upwelling. Sediment. Geol. 128, 179–199.

Sher, H.D. Martin, E.E. 2006. Timing and climate consequences of the opening of Drake Passage. Science 312, 5772. doi:10.1126/science.1120044.

Sher, H.D., Whittaker, J.M., Williams, S.e., Latimer, J.c., Kordesch, W.E.C., Delaney, M.L. 2015. Onset of Antarctic Circumpolar current 30 millions years ago as Tasmanian Gateway aligned with westerlies. Nature, 523, 580-583.do:10/1038/nature14598.

Shipley, T.H., Winterer, E.L., Lonsdale, P., 1983, Seismic-stratigraphic analysis in the pelagic environment: The central Hess Rise, Northwest Pacific, Mar. Geol. 51 (1-2), 47-62, https://doi.org/10.1016/0025-3227(83)90088-9.

Sleep, N.H.1990. Hotspot and mantle plumes: Some phenomenology. Journal of Geophysical Research: Solid Earth, 95, 6715-6736. doi.org/10.1029/JB095iB05p06715.

Smethie, W.M., Jr, Fine, R.A., Putzka, A., Jones, E.P. 2000. Tracing the flow of north Atlantic Deep Water using chlorofluorocarbons. Journal of Geophysical Research: Oceans, 105, C6, 14297-14323. doi.org/10.1029/1999JC90027.

Soares, D.M., Alves, T.M., Terrinha, P. 2014. Contourite drifts on early passive margins as an indicator of established lithosphere breakup, Earth Planet. Sci. Lett. 401, 116-131.

Southard, J.B., Young, R.A., Hollister, C.D. 1971. Experimental erosion of calcareous ooze. J. Geophysical Res. 76, 5903-5909.

Spencer-Cervato, C. 1998. Changing depth distribution of hiatuses during the Cenozoic. Paleoceanography, 13, 178-18.

Steele, J.H., Thorpe, S.A., Turekian, K.K. 2009. Elements of physical oceanography: A derivative of the Encyclopedia of Oceans. ISBN:9780123757258.

Stevenson, C.J., Talling, P.J., Wynn, R.B., Masson, D.G., Hunt, J.E., Frenz, M., Akhmetzhanhov, A., Cronin, B.T.2013. The flows that left no trace: Very large-volume turbidity currents that bypassed sediment through submarine channels without eroding the sea floor. Mar. Petrol. Geol. 41, 186-205. doi:10.1016/j.marpetgeo.2012.02.008.

Stow, D.A.V., Faugères, J.C., Howe, J.A., Pudsey, C.J., Viana, A., 2002. Contourites, bottom currents and deep-sea sediment drifts: current state-of-the-art. In: Stow, D.A.V., Pudsey, C.J., Howe, J.A., Faugères, J.C., Viana, A.R. (Eds.), Deep-Water Contourite Systems: Modern Drifts and Ancient Series, Seismic and Sedimentary Characteristics. Geological Society of London, Memoirs 22, pp. 7–20.

Stramma, L. 2001.Current systems in the Atlantic Ocean. In: Ocean currents: a derivative of the Encyclopedia of Ocean Sciences. (eds) J.H. Steele, S.A. Thorpe, K.K. Turekian. 718-727. doi:10.1006/rwos.2001.0360.

Straume, E.O., Gaina, C., Medvedev, S., Nisancioglu, K.H., 2020. Global Cenozoic Paleobathymetry with a focus on the Northern Hemisphere Oceanic Gateways. Gondwana Research, 86, 126-143. https://doi.org/10.1016/j.gr.2020.05.011.

Surlyk, F., Lykke-Andersen, H. 2007. Contourite drifts, moats and channels in the Upper Cretaceous chalk of the Danish Basin. Sedimentology 54, 405–422. doi: 10.1111/j.1365-3091.2006.00842.x.

Sykes, T.J.S., Ramsay, A.T.S., Kidd, R.B. 1998. Southern hemisphere Miocene bottom-water circulation: a paleobathymetric analysis. Geo. Soc. London Spec. Publ. vol131, 43-54, doi.org/10.1144/GSL.SP.1998.131.01.03.

Talling, P.J., Wynn, R.B., Masson, D.G., Frenz, M., Cronin, B.T., Schiebel, R., Akhmetzhanov, A.M., Dallmeier-Tiessen, S., Benetti, S., Weaver, P.P.E., Georgiopoulou, A., Zuhlsdorff, C., Amy, L.A. 2007. Onset of submarine debris flow deposition far from original giant landslide. Nature 450, 541-544.

Thran, A.C., Dutkiewicz, A., Spence, P., Dietmar Müller, R. 2018. Controls on the global distribution of contourite drifts: Insights from an eddy-resolving ocean model. Earth Planet. Sci. Lett. 489, 228–240. https://doi.org/10.1016/j.epsl.2018.02.044.

Thibault, N., Harlou, R., Schovsbo, N.H., Stemmerik, L., Surlyk. F. 2016. Late Cretaceous (late Campanian–Maastrichtian) sea-surface temperature record of the Boreal Chalk Sea. Clim. Past, 12, 429–438, 2016. doi:10.5194/cp-12-429-2016.

Thomas, D.J., Bralower, T.J., Jones, C.E. 2003. Neodymium isotopic reconstruction of late Paleocene-early Eocene thermohaline circulation. Earth Planet. Sci. Lett. 209, 309-322. doi:10.1016/S0012-821X(03)00096-7.

Toumoulin, A., Donnadieu, Y., Ladant, J.-B., Batenburg, S. J., Poblete, F., Dupont-Nivet, G. 2020. Quantifying the effect of the Drake Passage opening on the Eocene Ocean. Paleoceanography and Paleoclimatology, 35, e2020PA003889. https://doi.org/10.1029/2020PA003889.

Tuchiya, M., Talley, L.D., McCartney, M.S. 1992. An eastern Atlantic section from Iceland southward across the equator. Deep-Sea Res., 39, 1885-1917.

Tucholke, B.E. 2002. The Greater Antilles Outer Ridge: development of a distal sedimentary drift by deposition of fine-grained contourites. Stow, D. A. V., Pudsey, C. J., Howe, J. A., Faugères, J.-C., Viana, A. R. (eds) Deep-Water Contourite Systems: Modern Drifts and Ancient Series, Seismic and Sedimentary Characteristics. Geol. Soc. London Mem., 22, 39-55. 0435-4052/02/$15.00.

Tucholke, B. E., Ludwig, W. J. 1982. Structure and origin of the J Anomaly Ridge, western North Atlantic Ocean: Journal of Geophysical Research, v. 87, p. 9389-9407.

Tucholke, B. E., McCoy, F. W. 1986, Paleogeographic and paleobathymetric evolution of the North Atlantic Ocean; *in* Vogt, P. R., and Tucholke, B. E., eds., The Geology of North America, Volume M, The Western North Atlantic Region. Geol. Soc. Am., 589-602.

Tucholke, B.E., Vogt, P. et al 1979. Initial Reports of Deep Sea Drilling Project, Leg 43, Washington, D.C., U.S. Government Printing Office.

Uenzelmann-Neben, G., Gohl, K., Hochmuth, K., Salzmann, U., Larter, R.D., Hillenbrand, C-D., Klages, J. P. and Science Team of Expedition PS104. 2022. Deep water inflow slowed offshore expansion of the West Antarctic Ice Sheet at the Eocene-Oligocene transition. Communications Earth & Environment https://doi.org/10.1038/s43247-022-00369-x.

Vargas, J.M., Garcia-Lafuente, J., Delgado, J. Criado, F., 2003. Seasonal and wind-induced variability of Sea Surface Temperature patterns in the Gulf of Cadiz. Journal of Marine Systems 38 (3-4), 205-219.

Via, R.K., Thomas, D.J. 2006. Evolution of Atlantic thermohaline circulation: Early Oligocene onset of deep-water production in the North Atlantic. Geology 34, p. 441–444, doi: 10.1130/G22545.1.

Voigt, S., Jung, C., Friedrich, O., Frank, M., Teschner, C., Hoffmann, J. 2013. Tectonically restricted deep-ocean circulation at the end of the Cretaceous greenhouse. Earth Planet. Sci. Lett. 369-370, 169–177. http://dx.doi.org/10.1016/j.epsl.2013.03.019.

Wang, T., Lin, J., Tucholke, B., Chen, Y.J. 2011. Crustal thickness anomalies in the North Atlantic Ocean basin from gravity analysis, Geochem. Geophys. Geosyst., 12, Q0AE02, doi:10.1029/2010GC003402.

Wright, J.D., Miller, K.G., Fairbanks R.G. 1991. Evolution of deep-water circulation: Evidence from the Late Miocene Southern Ocean. Paleoceanography 6, 275-290.

Wright, J.D., Miller, K.G. 1993. Southern ocean influence on Late Eocene to Miocene deepwater circulation. The Antarctic Paleoenvironment: A perspective on global change. Part two, vol.60. doi.org/10.1002/9781118668061.ch1.

Wynn, R.B., Masson, D.G., Stow, D.A.V., Weaver, P.P.E. 2000. The Northwest African slope apron] a modern analogue for deep-water systems with complex seafloor topography. Mar. Petrol. Geol. 17, 253-265.

Zachos, J., Pagani, M., Sloan, L., Thomas, E., Billups, K. 2001. Trends, rhythms, and aberrations in global climate 65 Ma to present. Science 292, 686–693.

Zhang, Y., Grima, N., Huck, T. 2021. Fates of paleo-Antarctic Bottom Water during the early Eocene: Based on a Lagrangian analysis of IPSL-CM5A2 climate model simulations. Paleoceanography and Paleoclimatology, 36, e2019PA003845. https://doi.org/10.1029/2019PA003845.

Declaration of interests

☒The authors declare that they have no known competing financial interests or personal relationships that could have appeared to influence the work reported in this paper.

☐The authors declare the following financial interests/personal relationships which may be considered as potential competing interests:

HIGHLIGHTS

- Discovery of two contourite drift systems (CDS-1, CDS-2) in the Central NE-Atlantic.
- The CDS-1 recorded the circulation of SCW from Late Cretaceous to Miocene.
- The CDS-2 was formed by circulation of the AABW since the Miocene.